1-2015

Photonic-Loop Modeling Using Ghost Waveguides

Parikshit Dale

Photonic-Loop Modeling Using Ghost Waveguides

by

Parikshit Dale

A Thesis Submitted
in
Partial Fulfillment of the
Requirements for the Degree of
Master of Science
in
Telecommunication Engineering Technology

Supervised by

Dr. Drew Maywar

Department of Telecommunication Engineering Technology

College of Applied Science and Technology
Rochester Institute of Technology
Rochester, New York

January 2015

Dedication

To my family and my dearest friends:
Never have I been more grateful of your support, kindness and wisdom than in this moment.

I owe it all to you.

Acknowledgments

(goes in no particular order)

I would like to express enormous gratitude to my thesis adviser Prof. Drew Maywar. His guidance and motivation gave me desire to continue my education and confidence to pursue thesis. Prof. Maywar spent endless hours working with me on the research and answering all my questions. I would never have been able to complete my thesis without his continuous support, immense knowledge and enthusiasm.

Thank you to Prof. Mark Indelicato and Prof. Sung Young Kim for taking the time to be on my thesis committee.

I also want to thank all faculty and staff of the TET department who continuously helped and supported me through my education and made my time at RIT enjoyable and exciting.

I especially thank my family and friends who provided unconditional love, support, care and encouragement. I love them so much and deeply appreciate all they do for me.

Abstract

**Photonic-Loop Modeling Using
Ghost Waveguides**

Parikshit Dale

Supervising Professor: Dr. Drew Maywar

In this thesis, we present a new method for the modeling and analyzing photonic-loop structures which is based on a rotated directional coupler and ghost waveguide. This new method is less complicated than available methods. Our method of photonic-loop structure modeling is demonstrated by modeling and analyzing a ring resonator and its parameters. We also model and analyze a multi-ring ring resonator.

Contents

List of Figures

Chapter 1

Introduction

Without any doubt, innovation and advancement of integrated circuit (IC) was one of the important and revolutionary technical advancement in the twentieth century. The development of electronic ICs facilitates the ability to monolithically integrate multiple electronic devices into a single device providing many value-added functions by considerably reducing cost. Likewise a photonic integrated circuit (PIC), similar to electronic IC, on which many optical (sometimes electronic too) components are integrated and deliver an advancement related to cost, space, reliability and power. In PICs, optical components such as lasers, modulators, detectors, multiplexers, optical amplifiers, etc. are inter-linked to each other by optical couplers. So PICs are comprised of simple photonic devices to most complex photonic devices. Most of these photonic devices are comprised of simple or basic photonic devices. So in the course of design and development of photonic devices, it is essential to characterize the device parameters such as transmission parameters. If the device comprises some other basic devices then it is useful to conceptually divide the device to better understand its characteristics. Therefore different modeling techniques are used to analyze the behavior of active and passive photonic devices.

1.1 Modeling of Photonic Structures

Modeling of photonic circuits plays an important role in design and development of photonic devices. Therefore depending upon the stage of photonic device development, the modeling environment of photonics can be called as process modeling, device modeling or

circuit modeling.

- "Process modeling: covering both the numerical analysis of the fabrication process and equipment used for the fabrication." [4]
- "Device Modeling: the low-level analysis of the optical field inside an optical component as well as the analysis of the interaction with the electrical field in optoelectronic components." [4]
- "Circuit Modeling: the higher-level analysis of the operation of a set of devices connected within a photonic circuit." [4]

In view of the above modeling techniques, the thesis discusses about the device modeling of photonic loop structures and building blocks of photonic loop structures. The main objective of thesis is modeling of photonic loop structures using *ghost* waveguides.

1.2 Motivation and Scope of Thesis

As stated above, device modeling techniques are used for the analysis of optical fields inside an optical component. Some of the important quantities in the analysis of optical fields are the scattering matrix and transfer matrix along with the transmittivity and reflectivity.The scattering matrix and transfer matrix facilitates the relationship between the optical fields at different ports in the device. So these matrices play an important role in the analysis of optical fields in photonic devices. Transmittivity and reflectivity provides the transfer or reflection of power between specific ports.

Some methods are available to model photonic loop structures. So the thesis starts with the discussion of known methods to model photonic loop structures in chapter 2. Chapter 3 is focused on the directional coupler, a passive device, which is a major module in photonic loop structures. Chapter 3 is dedicated to the discussion about the formation of 2×2 transfer matrix from 2×2 scattering matrix in a four port unidirectional device and directional coupler. Chapter 4 talks about formation of a 2×2 transfer matrix from a 2×2 scattering

matrix in four port bidirectional device and rotated directional coupler. Chapter 5 discusses about parallel waveguides and their matrices. Chapter 6 discusses dual-waveguide ring resonator metrics as a result of the combination of rotated directional couplers with parallel waveguides. This chapter also validates the rotated directional coupler transfer matrix. Chapter 7 introduces the concept of *rotational directional coupler with ghost waveguide*. Chapter 7 advances with the application of *rotational directional coupler with ghost waveguide* concept in ring resonator.

1.3 Photonic Loop Structures

1.3.1 Building Blocks of Photonic Loop Structures

Among the wide assortment of photonic structures, some structures include loops of some form, including the photonic-ring resonator with single waveguide and dual waveguides. These photonic loop structures can be designed by some modifications in directional couplers with the help of photonic waveguides.

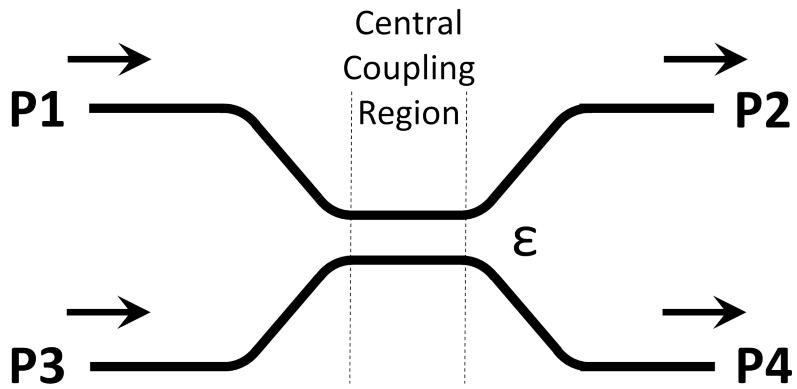

Figure 1.1: Directional Coupler

By connecting the different ports on opposite side of coupling region by photonic waveguide, different photonic loop structures can be designed. As seen in Fig. 1.1 the *directional coupler* has 4 ports in which two are input ports and two are output ports. Port

1 is the input port from which optical signal P1 goes into the directional coupler and propagates towards central coupling region. As light enters the central coupling region, a portion of it transmits out through port 2. This signal power is called as throughput power. Depending upon the central coupling region, a desired part of the input signal is coupled into the port 4. This port is called the coupled port. This device is termed as directional coupler (DC) since it directs the flow of light in desired direction. So directional couplers play a large role in photonic structures especially in photonic loop structures.

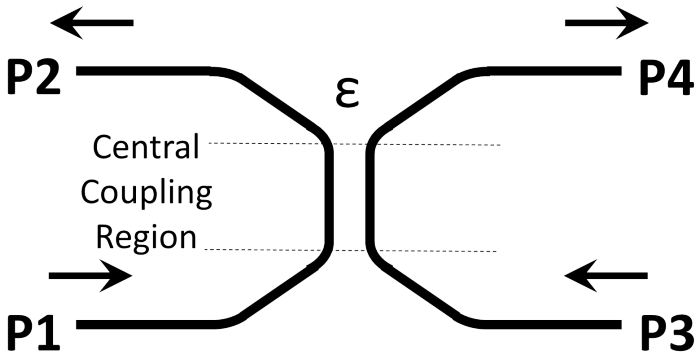

Figure 1.2: Rotated Directional Coupler

Fig. 1.2 is achieved by rotating the Fig. 1.1 by 90^o counter-clockwise. This device can be called as a *rotated directional coupler*.

The *rotated directional coupler* has 4 ports in which two are input ports and two are output ports. Port 1 is the input port from which optical signal P1 goes into the directional coupler and propagates towards central coupling region. As light enters the central coupling region, a portion of it transmits out through port 2. Depending upon the central coupling region, a desired part of the input signal is coupled into the port 4. So functionality of rotated directional coupler is same as directional coupler. The difference between the directional coupler and rotated directional coupler is the direction of light propagation. In the directional coupler, the light is traveling in the same direction in all ports, but in the rotated directional coupler the light is traveling in either the left to right or right to left direction. So the functionality of the rotated directional coupler remains the same as the

directional coupler but its application in modeling of photonic loop structures varies.My thesis discusses how this varied application plays a significant role in concept of modeling of photonic-loop structure using ghost waveguides.

Figure 1.3: Photonic Waveguide

Another basic but noteworthy component that performs a significant role in photonic loop structures is the *photonic waveguide*. It is a simple component with 2 ports, input port P1 and output port P2. Later chapters explores the significant role of photonic waveguides in the photonic loop structures.

The photonic directional coupler and photonic waveguide along with the photonic rotated directional coupler are basic elementary components for photonic-loop structures. So these components can be called as building blocks of photonic loop structures.

1.3.2 Photonic Loop Structures

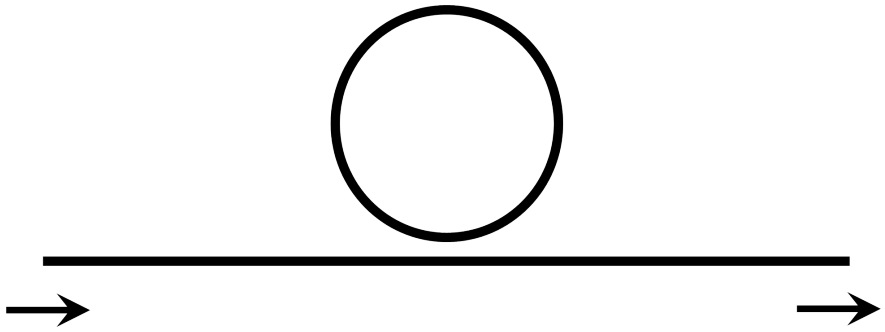

Figure 1.4: Photonic Ring Resonator

One photonic loop structure is the ring resonator shown in Fig. 1.4. The ring resonator is the most basic and generic configuration which consists of a unidirectional coupling between a ring resonator and a waveguide [11]. A ring resonator can be designed by placing

the photonic ring near the photonic waveguide creating coupling region between ring and waveguide. The principle characteristic of the ring resonator is that light propagates only in the forward direction. So sometimes it is also referred to as an all-pass filter.

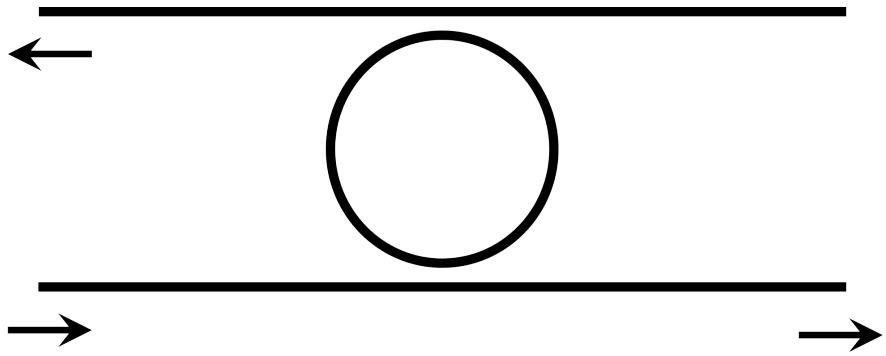

Figure 1.5: Dual-waveguide Photonic Ring Resonator

As seen in Fig. 1.5, by adding one more waveguide parallel to the waveguide in the ring resonator another type of photonic loop structure is formed. This structure is called a dual-waveguide resonator. Due to the addition of a waveguide, the light not only propagates in the forward direction but also drops at another port. This leads to major change of characteristic in ring resonator working. This filter is also referred as add-drop filter.

1.3.3 Modeling of Photonic-loop Structures

Some methods to model photonic-loop structures are known. One of such methods is of equating fields in the photonic-loop structures. Another known method is the unfolded equivalent system method [12]. Photonic-loop structures can be modeled using these methods but these methods get complicated or inefficient as the number of cascaded loops increases. These methods are discussed in chapter 2. My thesis introduces new method of modeling photonic-loop structures, using a concept of concatenation of building blocks of photonic-loop structures and the concept of ghost waveguides.

Chapter 2

Known Method to Model Photonic Loops

2.1 Method of Equating Fields

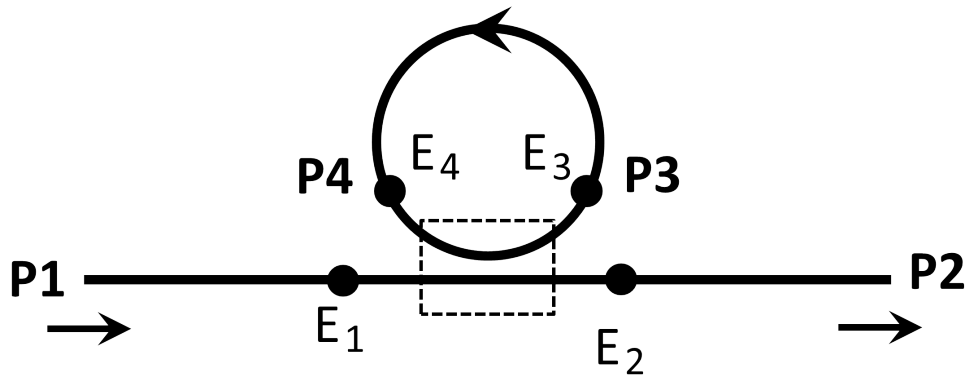

Figure 2.1: Photonic Ring Resonator

This method of the modeling photonic loops uses the concept of equating fields i.e. computing field at a specific port considering a different inputs and/or outputs field at a port. Lets consider the ring resonator with single waveguide shown in Fig. 2.1. In Fig. 2.1, the port P1 is the input port of the waveguide and the port P2 is the output port of the waveguide whereas the port P3 and P4 are ports on the ring. The coupling region between the ring and waveguide is same as coupling region of the directional coupler. When the optical light enters at the port P1, it propagates towards the coupling region. After entering the coupling region, the optical signal is split into two portions and enters the port P2 and P3. In the loop, the light within the port P3 circulates counter-clockwise and enters into the

port P4. The light from the port P4 and P1 combines in the coupling region and transmits through the port P2 and P3. So the light coming out of the port P2 is the combination of light from the port P1 and P4 and the light passing through P3 circulates in the ring generating resonances. Consider the coupling coefficient of the coupling region between the ring and the waveguide is ϵ i.e. from the port P1 to the port P3. So E_1,E_2, E_3 and E_4 denotes the field strengths of port P1, P2, P3 and P4 respectively. The field strengths E_1 and E_4 are combined together and are coupled to port P2 and P3 at the coupling region. So the field strength at the port P2 and P3 can be given as

$$E_2 = \sqrt{1-\epsilon}E_1 + \sqrt{\epsilon}E_4 \tag{2.1}$$

$$E_3 = \sqrt{\epsilon}E_1 + \sqrt{1-\epsilon}E_4 \tag{2.2}$$

This gives the electric field equations for the ring resonator. This is very simple method to derive electric field expressions for the ring resonator. But consider one more ring in the device as shown in Fig. 2.2. This device behaves similar as the ring resonator but not the same. Due to the addition of the ring, new coupling region is generated between two rings and this makes equating electric field difficult. To equate electric field in the 2-ring ring resonator, it is required to take splitting of light and resonances caused by the ring 2 into consideration. This makes modeling of 2-ring ring resonator complicated.

2.2 Method of Unfolded Equivalent System

The method of unfolded equivalent of the resonator in explained in Ref. [12]. In this method, the ring resonator shown in Fig. 2.1 is converted into Fig. 2.3. In this method, the ring resonator is unfolded by considering into two rings which are coupled by the Fabry-Perot(FP) etalon. The coupling region in the device equivalent is the directional coupler as mentioned above. So when the optical light enters the device, it propagated towards the coupling region. After entering the coupling region, the optical signal is split into two portions and some light is dissipated at the transmitted output while some of the light is

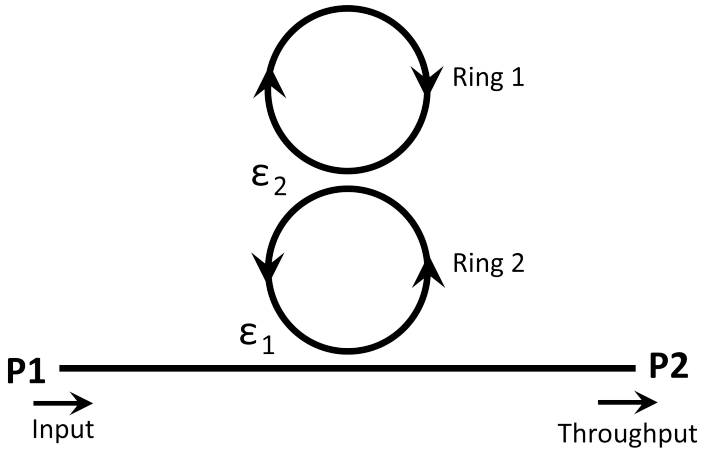

Figure 2.2: 2-Ring Ring Resonator

coupled into the ring 1. When the light traveling in counter clockwise direction reaches the FP etalon, some of the light continue to travel in ring while remaining light gets reflected by the FP etalon and travels in the ring 2 in counter clockwise direction. So in both rings, light travels in counter clockwise directions. The light traveling in the ring 1 in traveling through the FP etalon whereas the light in the ring 2 is traveling due to reflection at the FP etalon. "Thus the light always travels forward through the two rings; it is never considered to be reflected back into its own path." [12]

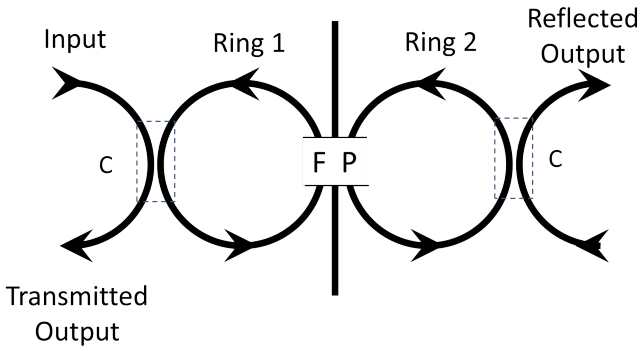

Figure 2.3: Unfolded Equivalent Model of Ring Resonator

The device is considered as the compound system in which the directional coupler is connected to the FT etalon by pair of fibers and the FP etalon is again connected to another

directional coupler by another pair of fibers. So the compound system has 5 components : 2 directional coupler, 2 pair of fibers and the FT etalon. The transfer matrix of the compound system shown in Fig. 2.3 is calculated using the transfer matrix method. The reflection coefficient R and the transmission coefficient T of the whole system are calculated by the transfer matrix. R and T equations carry the complex reflectance and transmittance of the FP etalon terms. Depending upon the amplitude reflection coefficient r of the mirrors of the FP etalon, functionality of the compound system varies. The value of r varies between 0 to 1. When value of r is neither 0 nor 1 then the compound system acts as a ring resonator. This method is also not much difficult and complex for the ring resonator.

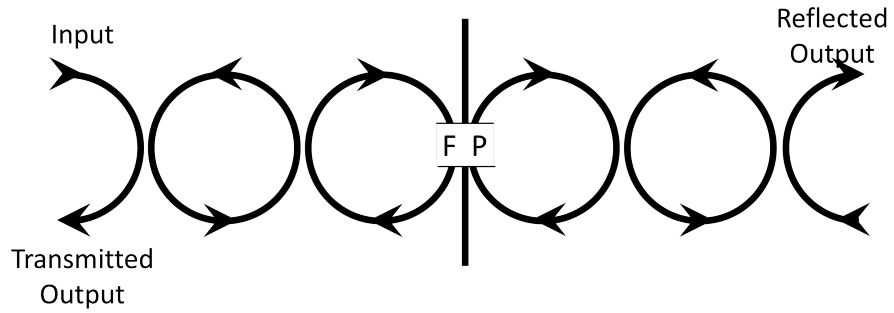

Figure 2.4: Unfolded Equivalent Model of 2-Ring Ring Resonator

Consider one more ring in the ring resonator as shown in Fig. 2.2. So unfolded equivalent model of the 2-ring ring resonator is as shown in Fig. 2.4. As seen in Fig. 2.4, unfolded equivalent model of the 2-ring ring resonator is a complex system with 4 directional couplers, 4 pairs of fibers and the FT etalon. So unfolding the device for equivalent model of the system is making the complex system more complex.

2.3 Summary of Known Method to Model Photonic Loops

The two known methods: the method of equating fields and the method of unfolded equivalent structures is discussed above. These two methods are uncomplicated for the simple structures like the ring resonator. But as the structures gets complicated like the 2-ring ring

resonator in Fig. 2.2, these two methods are gets complicated. So if the multiple rings are added in the ring resonator structure then theses methods will become very complicated.

Chapter 3

Directional Coupler

3.1 Four-Port Unidirectional Device

Four-port unidirectional devices contain four ports (two input and two output ports) and are unidirectional in nature. The unidirectional nature means that the light streams travel in only one direction. As shown in Fig. 3.1, four-port unidirectional devices are comprised of two input ports P1 and P3 and two output ports P2 and P4, and light traveling in the device is from the left to right direction.

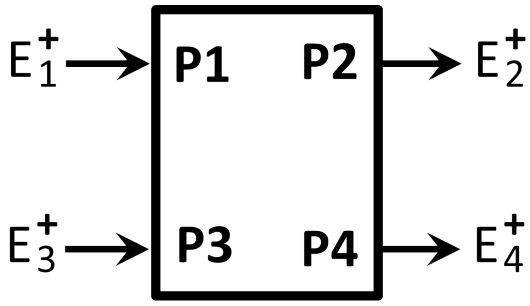

Figure 3.1: Four-Port Unidirectional Device

The electrical field strength at a port is denoted as E_x^y where,

x - Denotes the port number e.g. '1' for port P1

y - Denotes the direction of light stream. If the light stream is traveling from left to right at a port then y is '+' and if the light stream is traveling from right to left at a port then y is '-'.

E_1^+ ans E_3^+ denotes the input fields of port P1 and P3 whereas E_2^+ and E_4^+ denotes the

output fields of port P2 and P4. The total input in the device is denoted by *a* and the total output in the device is denoted by *b*. So input *a* and output *b* for Fig. 3.1 can be represented in matrix form as below:

$$a = \begin{bmatrix} E_1^+ \\ E_3^+ \end{bmatrix}, \tag{3.1}$$

$$b = \begin{bmatrix} E_2^+ \\ E_4^+ \end{bmatrix}. \tag{3.2}$$

In this thesis, all input and output matrices are written in a specific way. When writing matrices from top to bottom, the matrix parameters for the light stream traveling from left to right is written above the matrix parameters for light streams traveling from right to left. If both matrix parameters are representing light streams traveling in the same direction then matrix parameters for ports are written in a sequential manner from top port to bottom port in the device figure. In (3.1), in matrix for input *a*, E_1^+ and E_3^+ are traveling in the same direction. So E_1^+ and E_3^+ are written in a sequential manner from the top port to bottom port in the device shown in Fig. 3.1.

3.1.1 Scattering Matrix

A matrix which correlates the input states of a photonic device or system to the output state of a photonic device or system is known as *scattering matrix*. The scattering matrix *S* which correlates the coupling of optical field transfer from input *a* to output *b* is given as

$$b = Sa. \tag{3.3}$$

The parameters of scattering matrix *S*, which signify the optical field transfer coupling coefficients, are represented in the form of

$$s_{mn} = |s_{mn}| exp(i\phi_{mn}) \,,$$

where $|s_{mn}|$ correspond to the magnitude and ϕ_{mn} correspond to the phase difference from input port m to output port n. The correlation between input *a* in 3.1 and output *b* in 3.2 along with scattering matrix *S* for the *four* port *one* direction device in Fig. 3.1 is given as

$$\begin{bmatrix} E_2^+ \\ E_4^+ \end{bmatrix} = \begin{bmatrix} s_{12} & s_{32} \\ s_{14} & s_{34} \end{bmatrix} \begin{bmatrix} E_1^+ \\ E_3^+ \end{bmatrix}. \tag{3.4}$$

3.1.2 Formation of Transfer Matrix

Transfer matrix

Transfer characteristics of a photonic device can be defined by correlating the states on the left side of the coupling region to the states on the right side of the coupling region. This correlation can be given in terms of the *transfer matrix*. So the transfer matrix *T* for the *four* port *one* direction device in Fig. 3.1 is given as,

$$T = \begin{bmatrix} A & B \\ C & D \end{bmatrix}. \tag{3.5}$$

The correlation between the coefficients of states on the left side of the coupling region and the coefficients of states on the right side of the coupling region along with transfer matrix *T* for the *four* port *one* direction device in Fig. 3.1 is given as

$$\begin{bmatrix} E_2^+ \\ E_4^+ \end{bmatrix} = \begin{bmatrix} A & B \\ C & D \end{bmatrix} \begin{bmatrix} E_1^+ \\ E_3^+ \end{bmatrix}. \tag{3.6}$$

Formation of Transfer matrix

As the scattering matrix correlates the coefficients of the input state of a photonic device or system to the coefficients of the output state of a photonic device or system, it is comparatively straightforward to derive scattering matrix of a device than to derive transfer matrix

of a device. But in analysis and calculations transfer parameters of a device, transfer matrices are more appropriate than scattering matrices. So the scattering matrix can be derived initially and with the help of the scattering matrix, the transfer matrix can be derived. So in this section, the matrix formula for formation of a transfer matrix from a scattering matrix is derived.

From Fig. 3.1, it can be observed that all inputs are on the left side of the coupling region and all outputs are on the right side of coupling region. This observation is also seen in (3.4) and (3.6). So comparing (3.4) and (3.6), we get

$$\begin{bmatrix} A & B \\ C & D \end{bmatrix} = \begin{bmatrix} s_{12} & s_{32} \\ s_{14} & s_{34} \end{bmatrix}. \tag{3.7}$$

So the transfer matrix for the *four* port unidirectional device in Fig. 3.1 is written as

$$T = \begin{bmatrix} s_{12} & s_{32} \\ s_{14} & s_{34} \end{bmatrix} \tag{3.8}$$

3.1.3 Performance parameters

There are different performance parameters which provides some information about the device. Some of such performance parameters are explained below:

Transmittivity Transmittivity is the fraction of power transmitted from input port to the output port.

Reflectivity Reflectivity is the fraction of power reflected back to the same port.

Phase Transfer Functions Phase transfer functions are the phase differences between the input signal to the output signal after passing through a device.

Expansion of (3.6), gives following equations:

$$E_2^+ = AE_1^+ + BE_3^+, \tag{3.9}$$

$$E_4^+ = CE_1^+ + DE_3^+. \tag{3.10}$$

If light E_1^+ is launched at port P1 and input at port P3 is 0 , then substituting $E_3^+ = 0$ in the above equations gives the following equations:

$$E_2^+ = AE_1^+, \tag{3.11}$$

$$E_4^+ = CE_1^+. \tag{3.12}$$

Transmission coefficient τ_{12}

The transmission coefficient τ_{12} can be written as

$$\tau_{12} = \frac{E_2^+}{E_1^+}. \tag{3.13}$$

Restructuring (3.11), we get the following equation:

$$\frac{E_2^+}{E_1^+} = A. \tag{3.14}$$

From (3.7), $A = s_{12}$. So the transmission coefficient τ_{12} can be given as:

$$\tau_{12} = A = s_{12}. \tag{3.15}$$

Transmission coefficient τ_{14}

The transmission coefficient τ_{14} can be written as

$$\tau_{14} = \frac{E_4^+}{E_1^+}. \tag{3.16}$$

Restructuring (3.12), we get the following equation:

$$\frac{E_4^+}{E_1^+} = C. \tag{3.17}$$

From (3.7), $C = s_{14}$. So the transmission coefficient τ_{14} can be given as:

$$\tau_{14} = C = s_{14}. \tag{3.18}$$

3.2 Directional Coupler

3.2.1 Introduction

As described in 1.3.1, a directional coupler is a four port device and light is traveling in only one direction. So a directional coupler can be considered as a four-port unidirectional device.

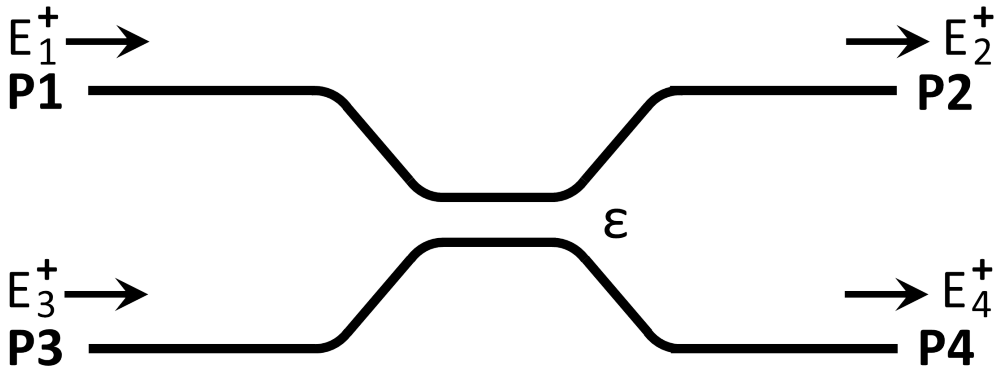

Figure 3.2: Directional Coupler

As shown in Fig. 3.2, a directional coupler consists of four ports P1, P2, P3 and P4. Ports P1 and P3 act as input ports and ports P2 and P4 act as output ports. E_1^+ ans E_3^+ denote the input field strengths of port P1 and P3. E_2^+ and E_4^+ denotes the output field strength of port P2 and P4. So input *a* and output *b* for Figure 3.2 are given as,

$$a = \begin{bmatrix} E_1^+ \\ E_3^+ \end{bmatrix}, \tag{3.19}$$

$$b = \begin{bmatrix} E_2^+ \\ E_4^+ \end{bmatrix}. \tag{3.20}$$

3.2.2 Scattering Matrix

As mentioned in 3.1.1, the scattering matrix correlates the coefficients of the input state of a photonic device or system to the coefficients of the output state of a photonic device or system. So from (3.3), the scattering matrix *S* which correlates the coupling of optical fields from input *a* to output *b* is given as

$$b = Sa. \tag{3.21}$$

From (3.19), (3.20) and (3.21), the correlation between input, output and scattering matrix S for the directional coupler in Figure 3.2 is given as

$$\begin{bmatrix} E_2^+ \\ E_4^+ \end{bmatrix} = \begin{bmatrix} s_{12} & s_{32} \\ s_{14} & s_{34} \end{bmatrix} \begin{bmatrix} E_1^+ \\ E_3^+ \end{bmatrix} \tag{3.22}$$

By expansion of the above equation, we get

$$E_2^+ = s_{12}E_1^+ + s_{32}E_3^+, \tag{3.23}$$

$$E_4^+ = s_{14}E_1^+ + s_{34}E_3^+. \tag{3.24}$$

The scattering matrix *S* has two restrictions when we consider an actual physical device [5]. The restrictions are:

1. “The first restriction is the result of the reciprocity condition arising from the fact that Maxwell’s equation are invariant for time inversion. It means that they have two

solutions in opposite propagating directions through the device, assuming single-mode operation."

$$s_{14} = s_{32}. \tag{3.25}$$

2. Consider the device as a lossless device. So according to the energy-conservation principle, the total of the energy at inputs must match the total of energy at outputs. This is given as [5]

$$E^{\dagger}_{output} E_{output} = E^{\dagger}_{input} E_{input},$$

where, superscript † denotes the transpose conjugate. This equation can also be written as,

$$E_2^+(E_2^+)^* + E_4^+(E_4^+)^* = E_1^+(E_1^+)^* + E_3^+(E_3^+)^*, \tag{3.26}$$

where superscript $*$ denotes the complex conjugate.

The complex conjugate of (3.23) and (3.24) is given as

$$(E_2^+)^* = s_{12}^*(E_1^+)^* + s_{32}^*(E_3^+)^*, \tag{3.27}$$

$$(E_4^+)^* = s_{14}^*(E_1^+)^* + s_{34}^*(E_3^+)^*. \tag{3.28}$$

By multiplication of (3.23) and (3.27), we get

$$\begin{aligned} E_2^+(E_2^+)^* &= (s_{12}E_1^+ + s_{32}E_3^+)(s_{12}^*(E_1^+)^* + s_{32}^*(E_3^+)^*) \\ &= s_{12}s_{12}^*E_1^+(E_1^+)^* + s_{12}s_{32}^*E_1^+(E_3^+)^* + \\ &\quad s_{32}s_{12}^*E_3^+(E_1^+)^* + s_{32}s_{32}^*E_3^+(E_3^+)^*. \end{aligned} \tag{3.29}$$

By multiplication of (3.24) and (3.28), we get

$$\begin{aligned} E_4^+(E_4^+)^* &= (s_{14}E_1^+ + s_{34}E_3^+)(s_{14}^*(E_1^+)^* + s_{34}^*(E_3^+)^*) \\ &= s_{14}s_{14}^*E_1^+(E_1^+)^* + s_{14}s_{34}^*E_1^+(E_3^+)^* + \\ &\quad s_{34}s_{14}^*E_3^+(E_1^+)^* + s_{34}s_{34}^*E_3^+(E_3^+)^*. \end{aligned} \tag{3.30}$$

By addition of (3.29) and (3.30), we get

$$\begin{aligned} E_2^+(E_2^+)^* + E_4^+(E_4^+)^* &= s_{12}s_{12}^* E_1^+(E_1^+)^* + s_{12}s_{32}^* E_1^+(E_3^+)^* + s_{32}s_{12}^* E_3^+(E_1^+)^* + s_{32}s_{32}^* E_3^+(E_3^+)^* \\ &\quad + s_{14}s_{14}^* E_1^+(E_1^+)^* + s_{14}s_{34}^* E_1^+(E_3^+)^* + s_{34}s_{14}^* E_3^+(E_1^+)^* + s_{34}s_{34}^* E_3^+(E_3^+)^* \\ &= (s_{12}s_{12}^* + s_{14}s_{14}^*)E_1^+(E_1^+)^* + (s_{12}s_{32}^* + s_{14}s_{34}^*)E_1^+(E_3^+)^* \\ &\quad + (s_{32}s_{12}^* + s_{34}s_{14}^*)E_3^+(E_1^+)^* + (s_{32}s_{32}^* + s_{34}s_{34}^*)E_3^+(E_3^+)^*. \end{aligned} \tag{3.31}$$

By comparison of (3.26) and (3.31),

$$\begin{aligned} (s_{12}s_{12}^* + s_{14}s_{14}^*)E_1^+(E_1^+)^* &= E_1^+(E_1^+)^*, \\ (s_{12}s_{32}^* + s_{14}s_{34}^*)E_1^+(E_3^+)^* &= 0, \\ (s_{32}s_{12}^* + s_{34}s_{14}^*)E_3^+(E_1^+)^* &= 0, \\ (s_{32}s_{32}^* + s_{34}s_{34}^*)E_3^+(E_3^+)^* &= E_3^+(E_3^+)^*. \end{aligned} \tag{3.32}$$

Solving the above equations, and substituting $s_{14} = s_{32}$ from (3.25), we get

$$s_{12}s_{12}^* + s_{14}s_{14}^* = 1, \tag{3.33}$$

$$s_{32}s_{12}^* + s_{34}s_{32}^* = 0, \tag{3.34}$$

$$s_{32}s_{32}^* + s_{34}s_{34}^* = 1. \tag{3.35}$$

The directional coupler is devised such that some quantity of power from input port 1 is dissipated at output port 2 while the remaining quantity of power is dissipated at output port 4. Consider ϵ as the optical power transfer coupling coefficient from input 1 to output 4. So the remaining of optical power $(1 - \epsilon)$ from input port 1 is dissipated at output port 2. Assume that, without loss of generality, the phase difference between the electric field from input port 1 and output port 2, ϕ_{12}, is zero. So the element of the scattering matrix,s_{12},

which represent the optical field transfer coupling coefficient from input port 1 to output port 2 is given by

$$\begin{aligned} s_{12} &= |\sqrt{1-\epsilon}|exp(j0), \\ s_{12} &= \sqrt{1-\epsilon}. \end{aligned} \tag{3.36}$$

Assume that the coupler is symmetric. So the optical power transfer coupling coefficient s_{34} from input port 3 to output port 4 is equivalent to s_{12} with phase difference of zero i.e.$\phi_{34} = 0$:

$$\begin{aligned} s_{34} &= |\sqrt{1-\epsilon}|exp(j0), \\ s_{34} &= \sqrt{1-\epsilon}. \end{aligned} \tag{3.37}$$

As ϵ is the optical power transfer coupling coefficient from input 1 to output 4 as well as from input 3 to output 4,the magnitude of s_{32} is equivalent to s_{14}, i.e. $\sqrt{\epsilon}$. Assume that the phase difference between input port 3 and output port 2 is ϕ_{32}:

$$\begin{aligned} s_{32} &= |\sqrt{\epsilon}|exp(j\phi_{32}), \\ &= \sqrt{\epsilon}exp(j\phi_{32}). \end{aligned} \tag{3.38}$$

Substituting values from (3.36), (3.37) and (3.38) into (3.34),

$$\begin{aligned} \sqrt{\epsilon}exp(j\phi_{32})\sqrt{1-\epsilon} + \sqrt{1-\epsilon}\sqrt{\epsilon}(exp(j\phi_{32}))^* &= 0, \\ \sqrt{\epsilon}exp(j\phi_{32})\sqrt{1-\epsilon} + \sqrt{1-\epsilon}\sqrt{\epsilon}exp(-j\phi_{32}) &= 0, \\ exp(j\phi_{32}) + exp(-j\phi_{32}) &= 0. \end{aligned}$$

By Euler's formula

$$cos(j\phi_{32}) + jsin(j\phi_{32}) + cos(-j\phi_{32}) + jsin(-j\phi_{32}) = 0,$$
$$cos(j\phi_{32}) + cos(j\phi_{32}) = 0,$$
$$cos(j\phi_{32}) = 0.$$

Solving the above equation

$$\phi_{32} = (2n+1)\frac{\pi}{2}, \tag{3.39}$$

where, n = 0,1,2,3...

Substitute the above value in (3.38), we get

$$\begin{aligned} s_{32} &= |\sqrt{\epsilon}|exp\left(j\frac{\pi}{2}\right), \\ &= j\sqrt{\epsilon}. \end{aligned} \tag{3.40}$$

But from (3.25), $s_{14} = s_{32}$. So s_{14} is written as

$$s_{14} = j\sqrt{\epsilon}. \tag{3.41}$$

Substituting values from (3.36), (3.37), (3.40) and (3.41) in (3.22), the scattering matrix for the directional coupler is given as

$$S = \begin{bmatrix} \sqrt{1-\epsilon} & j\sqrt{\epsilon} \\ j\sqrt{\epsilon} & \sqrt{1-\epsilon} \end{bmatrix}. \tag{3.42}$$

3.2.3 Formation of transfer matrix

The transfer matrix fora *four* port *one* direction device is derived in 3.1.2. (3.1.2) provides a formula to derive the transfer matrix from the scattering matrix for a *four* port *one* direction device. As previously mentioned, the directional coupler is a *four* port *one* direction device, and so transfer matrix for directional coupler can be derived by comparison of (3.1.2) and (3.42). So the transfer matrix for a directional coupler can be written as:

$$T = \begin{bmatrix} \sqrt{1-\epsilon} & j\sqrt{\epsilon} \\ j\sqrt{\epsilon} & \sqrt{1-\epsilon} \end{bmatrix}. \tag{3.43}$$

3.2.4 Transmittivity and Phase Transfer Functions

Transmission Coefficient τ_{12}

The transmission coefficient τ_{12} for a *four* port *one* direction device is derived in 3.1.3. From (3.15), the transmission coefficient τ_{12} for a directional coupler can be written as:

$$\tau_{12} = A.$$

We calculate the value of A by comparing (3.5) and (3.43), and substituting it in the above equation gives the transmission coefficient τ_{12} for a directional coupler:

$$\tau_{12} = \sqrt{1-\epsilon}. \tag{3.44}$$

So the transmission coefficient τ_{12} of a directional coupler is $\sqrt{1-\epsilon}$.

Transmission Coefficient τ_{14}

The transmission coefficient τ_{14} for a *four* port *one* direction device is derived in 3.1.3. From (3.18), the transmission coefficient τ_{14} for a directional coupler can be written as:

$$\tau_{14} = C.$$

We calculate the value of A by comparing (3.5) and (3.43), and substituting it in the above equation gives the transmission coefficient τ_{14} for a directional coupler:

$$\tau_{14} = j\sqrt{\epsilon}. \tag{3.45}$$

So the transmission coefficient τ_{14} of a a directional coupler is $j\sqrt{\epsilon}$.

Transmittivity T_{12}

As the transmittivity T_{12} is the fraction of power transmitted from input port P1 to the output port P2 passing through the coupling region of a a directional coupler, it is calculated from the transmission coefficient τ_{12} as follow,

$$\begin{aligned} T_{12} &= |\tau_{12}|^2, \\ T_{12} &= \tau_{12} * \tau_{12}^*, \\ T_{12} &= \sqrt{1-\epsilon} * (\sqrt{1-\epsilon^*})^*, \\ T_{12} &= \sqrt{1-\epsilon} * \sqrt{1-\epsilon^*}, \\ T_{12} &= (1-\epsilon). \end{aligned} \tag{3.46}$$

So the transmittivity T_{12} of a a directional coupler is $(1-\epsilon)$.

Transmittivitty T_{14}

As the transmittivity T_{14} is the fraction of power transmitted from input port P1 to the output port P4 passing through the coupling region of a a directional coupler, it is calculated from the transmission coefficient τ_{14} as follow,

$$\begin{aligned} T_{14} &= |\tau_{14}|^2, \\ T_{14} &= \tau_{14} * \tau_{14}^*, \\ T_{14} &= j\sqrt{\epsilon} * (j\sqrt{\epsilon})^*, \\ T_{14} &= j\sqrt{\epsilon} * (-j\sqrt{\epsilon}), \\ T_{14} &= \epsilon. \end{aligned} \tag{3.47}$$

So the transmittivity T_{14} of a a directional coupler is ϵ.

Transmittivity vs. ϵ Spectra

As seen in (3.46) and (3.47), the transmittivity of a directional coupler is dependent upon ϵ. The graph in Fig. 3.3 shows how the transmittivity T_{12} and T_{14} varies with ϵ. As seen in Fig. 3.3, T_{12} decreases as ϵ increases whereas T_{14} increases with ϵ.

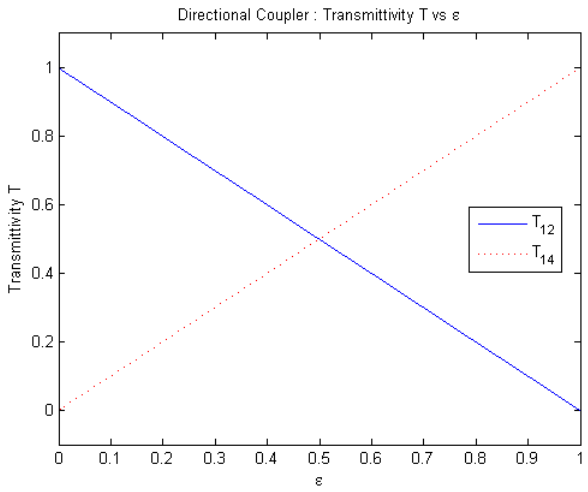

Figure 3.3: the transmittivity vs. ϵ

Phase Transfer Function ϕ_{12}

As the phase transfer function ϕ_{12} is the phase difference between the input at port P1 to the output at port P2 after passing through coupling region of coupler, it is calculated from the transmission coefficient τ_{12} as follow,

$$\begin{aligned}
\phi_{12} &= arg(\tau_{12}), \\
\phi_{12} &= arg(\sqrt{1-\epsilon}), \\
\phi_{12} &= tan^{-1}\left(\frac{0}{\sqrt{1-\epsilon}}\right), \\
\phi_{12} &= 0.
\end{aligned} \tag{3.48}$$

So the phase transfer function ϕ_{12} of a a directional coupler is 0.

Phase Transfer Function ϕ_{14}

As the phase transfer function ϕ_{14} is the phase difference between the input at port P1 to the output at port P4 after passing through coupling region of coupler, it is calculated from the transmission coefficient τ_{14} as follow,

$$\begin{aligned}
\phi_{14} &= arg(\tau_{14}), \\
\phi_{14} &= arg(j\sqrt{\epsilon}), \\
\phi_{14} &= tan^{-1}\left(\frac{\sqrt{\epsilon}}{0}\right), \\
\phi_{14} &= \frac{\pi}{2}.
\end{aligned} \tag{3.49}$$

So the phase transfer function ϕ_{14} of a a directional coupler is $\frac{\pi}{2}$.

Phase Transfer Function vs. ϵ Spectra

As seen in (3.48) and (3.48), the phase transfer function of a directional coupler is not dependent upon ϵ. The graph in Fig. 3.4 shows that even as ϵ changes, the phase transfer function ϕ_{12} and ϕ_{14} remains same. As seen in Fig. 3.4, ϕ_{12} is 0 and ϕ_{14} is $\frac{\pi}{2}$ for all values of ϵ.

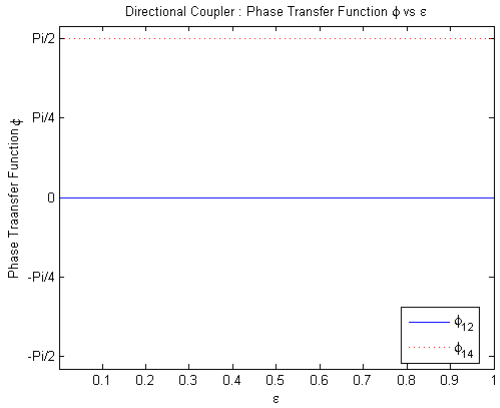

Figure 3.4: Phase Transfer Function vs. ϵ

3.2.5 Conservation of Power

Conservation of a power means that for a lossless device, the total amount of power in a system remains constant despite changes inside a system.So for a lossless device, the total amount of input power must be equal to total amount of output power as there is no loss in device. As the transmittivity is the fraction of power transmitted from the input port to the output port passing through the coupling region of coupler and the reflectivity is the fraction of power reflected back to the same port passing through the coupling region of a coupler, the total of all the transmittivity and reflectivity of a device must be equal to 1.

Above, we considered input only at port P1 and we considered input at port P3 as 0. So power from port P1 is transmitted to only port P2 and port P4 as as there is no coupling between input port P1 to port P3 and there is no reflection at port P1. As stated the above, for conservation of power in a lossless directional coupler, the total of the transmittivity T_{12} and the transmittivity T_{14} must be 1.

$$\begin{aligned} T_{Total} &= T_{12} + T_{14}, \\ T_{Total} &= 1 - \epsilon + \epsilon, \\ T_{Total} &= 1. \end{aligned} \tag{3.50}$$

As the total the transmittivity is equal to 1, the is conservation of power in a lossless directional coupler.

3.2.6 Unitaryness of a Transfer Matrix

A square matrix U is unitary if

$$U^H = U^{-1}, \tag{3.51}$$

where U^H denotes the conjugate transpose and U^{-1} is the matrix inverse.

So to verify that the transfer matrix for a directional coupler with unidirectional waveguides is a unitary matrix, we calculate and compare conjugate transpose and matrix inverse of the transfer matrix. Conjugate transpose is as below:

$$T^H = \begin{bmatrix} \sqrt{1-\epsilon} & -j\sqrt{\epsilon} \\ -j\sqrt{\epsilon} & \sqrt{1-\epsilon} \end{bmatrix} \tag{3.52}$$

Also the inverse of the transfer matrix is given as below:

$$T^{-1} = \begin{bmatrix} \sqrt{1-\epsilon} & -j\sqrt{\epsilon} \\ -j\sqrt{\epsilon} & \sqrt{1-\epsilon} \end{bmatrix} \tag{3.53}$$

Comparing (3.52) and (3.53), we get that

$$T^H = T^{-1} \tag{3.54}$$

So the transfer matrix of a directional coupler with unidirectional waveguides is a unitary matrix.

3.2.7 Determinant of a Transfer Matrix

The determinant of the transfer matrix of a directional coupler with unidirectional waveguides is given as below:

$$\begin{aligned} det(T) &= \begin{vmatrix} \sqrt{1-\epsilon} & j\sqrt{\epsilon} \\ j\sqrt{\epsilon} & \sqrt{1-\epsilon} \end{vmatrix}, \\ det(T) &= \sqrt{1-\epsilon}\sqrt{1-\epsilon} - j\sqrt{\epsilon}j\sqrt{\epsilon} \\ det(T) &= 1 - \epsilon + \epsilon, \\ det(T) &= 1. \end{aligned} \tag{3.55}$$

So the determinant of a symmetric lossless directional coupler with unidirectional waveguides is 1.

Chapter 4

Rotated Directional Coupler

4.1 Four Port Bidirectional Device

Four-port bidirectional device contains four ports (two input and two output ports) and device is bidirectional in nature. The bidirectional nature of device means that the light streams traveling in ports in the device are in either left to right or right to left direction. As shown in Fig. 4.1, four port unidirectional devices comprises of two input ports P1 and P2 and two output ports P3 and P4, and the light traveling in device is in left to right direction at ports P1 and P4 and in right to left direction at port P2 and P3.

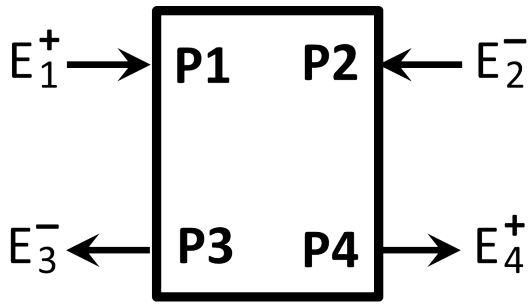

Figure 4.1: Four-Port Bnidirectional Device

E_1^+ ans E_2^- denotes the input field strengths of port P1 and P2 whereas E_3^- and E_4^+ denotes the output field strengths of port P3 and P4. The total input in the device is denoted by *a* and the total output in the device is denoted by *b*. So the input *a* and the output *b* for Fig. 4.1 can be represented in matrix form as below:

$$a = \begin{bmatrix} E_1^+ \\ E_2^- \end{bmatrix}, \tag{4.1}$$

$$b = \begin{bmatrix} E_4^+ \\ E_3^- \end{bmatrix}. \tag{4.2}$$

4.1.1 Scattering Matrix

As mentioned in 3.1.1, the scattering matrix correlates the coefficients of the input state of a photonic device or system to the coefficients of the output state of a photonic device or system. So from (3.3), the scattering matrix *S* which correlates the coupling of optical power transfer from the input *a* to the output *b* is given as

$$b = Sa. \tag{4.3}$$

The correlation between the input *a* in 4.1 and the output *b* in 4.2 along with the scattering matrix *S* for the *four* port *two* directional device in Fig. 4.1 is given as

$$\begin{bmatrix} E_4^+ \\ E_3^- \end{bmatrix} = \begin{bmatrix} s_{14} & s_{24} \\ s_{13} & s_{23} \end{bmatrix} \begin{bmatrix} E_1^+ \\ E_2^- \end{bmatrix}. \tag{4.4}$$

4.1.2 Formation of Transfer Matrix

Transfer Matrix

As mentioned in 3.1.2, the *transfer matrix* correlates the coefficients of states on the left side of the coupling region to the coefficients of states on the right side of the coupling region. So the transfer matrix *T* for the *four* port *two* direction device in Fig. 4.1 is given as

$$T = \begin{bmatrix} A & B \\ C & D \end{bmatrix}, \tag{4.5}$$

The correlation between the coefficients of states on the left side of the coupling region and the coefficients of states on the right side of the coupling region along with the transfer matrix *T* for the *four* port *two* direction device in Fig. 4.1 is given as

$$\begin{bmatrix} E_4^+ \\ E_2^- \end{bmatrix} = \begin{bmatrix} A & B \\ C & D \end{bmatrix} \begin{bmatrix} E_1^+ \\ E_3^- \end{bmatrix} \tag{4.6}$$

Formation of Transfer Matrix

As stated in chapter 3, in analysis and calculations transfer parameters of a device, transfer matrices are more appropriate than the scattering matrices. So the scattering matrix can be derived initially and with the help of the scattering matrix, the transfer matrix can be derived. So in this section, matrix formula for formation of the transfer matrix from the scattering matrix is derived.

From Fig. 4.1 and (4.6), it can be observed that one input and one output is on either side of a coupling region. So for formation of the transfer matrix from the scattering matrix, it is obligatory to expand and rearrange the scattering matrix in 4.4. By expansion of 4.4, we get the following equations,

$$E_4^+ = s_{14}E_1^+ + s_{24}E_2^-, \tag{4.7}$$

$$E_3^- = s_{13}E_1^+ + s_{23}E_2^-. \tag{4.8}$$

Rearranging (4.8), we get

$$\begin{aligned} E_3^- &= s_{13}E_1^+ + s_{23}E_2^-, \\ s_{23}E_2^- &= -s_{13}E_1^+ + E_3^-, \\ E_2^- &= -\frac{s_{13}}{s_{23}}E_1^+ + \frac{1}{s_{23}}E_3^-. \end{aligned} \tag{4.9}$$

Substitute value of E_2^- in (4.7),

$$\begin{aligned}
E_4^+ &= s_{14}E_1^+ + s_{24}\left[-\frac{s_{13}}{s_{23}}E_1^+ + \frac{1}{s_{23}}E_3^-\right], \\
E_4^+ &= s_{14}E_1^+ - \frac{s_{24}s_{13}}{s_{23}}E_1^+ + \frac{s_{24}}{s_{23}}E_3^-, \\
E_4^+ &= s_{14}E_1^+ - \frac{s_{24}s_{13}}{s_{23}}E_1^+ + \frac{s_{24}}{s_{23}}E_3^-, \\
E_4^+ &= \frac{s_{14}s_{23} - s_{24}s_{13}}{s_{23}}E_1^+ + \frac{s_{24}}{s_{23}}E_3^-. \qquad (4.10)
\end{aligned}$$

By arranging (4.9) and (4.10) in matrix form, we get

$$\begin{bmatrix} E_4^+ \\ E_2^- \end{bmatrix} = \frac{1}{s_{23}} \begin{bmatrix} s_{14}s_{23} - s_{24}s_{13} & s_{24} \\ -s_{13} & 1 \end{bmatrix} \begin{bmatrix} E_1^+ \\ E_3^- \end{bmatrix}. \qquad (4.11)$$

The (4.11) is similar to (4.6). So the *transfer matrix* for *four* port *two* direction device in Fig. 4.1 is written as

$$T = \frac{1}{s_{23}} \begin{bmatrix} s_{14}s_{23} - s_{24}s_{13} & s_{24} \\ -s_{13} & 1 \end{bmatrix}. \qquad (4.12)$$

4.1.3 Transmission Parameters

As mentioned in previous chapter, transmission parameters provides some information about transmission of power in device. By expansion of (4.6), we get the following equations,

$$E_4^+ = AE_1^+ + BE_3^-, \qquad (4.13)$$

$$E_2^- = CE_1^+ + DE_3^-. \qquad (4.14)$$

If the light E_1^+ is launched at port P1 and the input at port P2 is 0 , then substituting $E_2^- = 0$ in the above equations gives the following equations:

$$E_4^+ = AE_1^+ + BE_3^-, \tag{4.15}$$

$$0 = CE_1^+ + DE_3^-. \tag{4.16}$$

Transmission Coefficient τ_{13}

Transmission coefficient τ_{13} can be written as

$$\tau_{13} = \frac{E_3^-}{E_1^+}. \tag{4.17}$$

Restructuring (4.16), we get the following equation:

$$DE_3^- = -CE_1^+,$$

$$E_3^- = -\frac{C}{D}E_1^+, \tag{4.18}$$

$$\frac{E_3^-}{E_1^+} = -\frac{C}{D}, \tag{4.19}$$

$$\tau_{13} = -\frac{C}{D}. \tag{4.20}$$

So transmission coefficient τ_{13} can be given as $-\frac{C}{D}$.

Transmission Coefficient τ_{14}

Transmission coefficient τ_{14} can be written as

$$\tau_{14} = \frac{E_4^+}{E_1^+}. \tag{4.21}$$

Substitute value of E_3^- from (4.18) into (4.15), we get the following equation:

$$E_4^+ = AE_1^+ + B\left[-\frac{C}{D}E_1^+\right],$$
$$E_4^+ = AE_1^+ - \frac{BC}{D}E_1^+,$$
$$E_4^+ = \frac{AD-BC}{D}E_1^+, \tag{4.22}$$
$$\frac{E_4^+}{E_1^+} = \frac{AD-BC}{D}, \tag{4.23}$$
$$\tau_{14} = \frac{AD-BC}{D}. \tag{4.24}$$

So transmission coefficient τ_{14} can be given as $-\frac{AD-BC}{D}$.

4.2 Rotated Directional Coupler

4.2.1 Introduction

As described in 1.3.1, rotated directional coupler is four port device and the light is traveling in ports in the device are in either left to right or right to left direction . So rotated directional coupler can be considered as a four port bidirectional device.

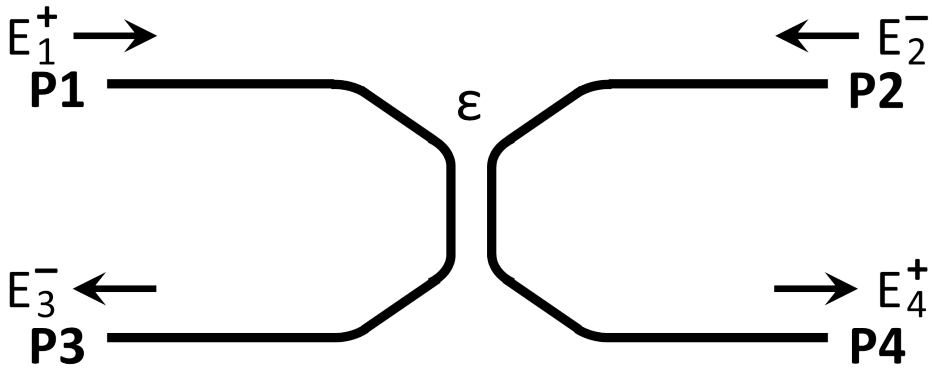

Figure 4.2: Rotated Directional Coupler

As shown in Fig. 4.2, rotated directional coupler comprises of four ports P1, P2, P3 and P4. Ports P1 and P2 acts as the input port and ports P3 and P4 acts as the output port. E_1^+

ans E_2^- denotes the input field strengths of port P1 and P2. E_3^- and E_4^+ denotes the output field strengths of port P3 and P4. So the input *a* and the output *b* for Figure 4.2 is given as

$$a = \begin{bmatrix} E_1^+ \\ E_2^- \end{bmatrix}, \tag{4.25}$$

$$b = \begin{bmatrix} E_4^+ \\ E_3^- \end{bmatrix}. \tag{4.26}$$

4.2.2 Scattering Matrix

As mentioned in 3.1.1, the scattering matrix correlates the coefficients of the input state of a photonic device or system to the coefficients of the output state of a photonic device or system. So from (3.3), the scattering matrix *S* which correlates the coupling of optical power transfer from the input *a* to the output *b* is given as

$$b = Sa. \tag{4.27}$$

From (4.25), (4.26) and (4.27), correlation between the input, the output and the scattering matrix S for the directional coupler in Figure 4.2 is given as

$$\begin{bmatrix} E_4^+ \\ E_3^- \end{bmatrix} = \begin{bmatrix} s_{14} & s_{24} \\ s_{13} & s_{23} \end{bmatrix} \begin{bmatrix} E_1^+ \\ E_2^- \end{bmatrix}. \tag{4.28}$$

As mentioned in 1.3.1, functionality of rotated directional coupler is same as directional coupler. The difference between directional coupler and rotated directional coupler is direction of the light stream traveling in ports. But direction of the light has no effect on transfer of power in the device. So the above equation represents the light stream traveling from top to bottom in directional coupler where the output is on the left side and the input is on the right side of equation. So the above equation is same as the scattering matrix of directional coupler. By comparison of (3.42) and (4.28), we get,

$$\begin{bmatrix} s_{14} & s_{24} \\ s_{13} & s_{23} \end{bmatrix} = \begin{bmatrix} \sqrt{1-\epsilon} & j\sqrt{\epsilon} \\ j\sqrt{\epsilon} & \sqrt{1-\epsilon} \end{bmatrix}. \tag{4.29}$$

So the scattering matrix for rotated directional coupler is written as

$$S = \begin{bmatrix} \sqrt{1-\epsilon} & j\sqrt{\epsilon} \\ j\sqrt{\epsilon} & \sqrt{1-\epsilon} \end{bmatrix}. \tag{4.30}$$

4.2.3 Formation of Transfer Tatrix

The transfer matrix for *four* port *two* direction device is derived in 4.1.2. (4.12) provides a formula to derive the transfer matrix from the scattering matrix for *four* port *two* direction device. As previously mentioned, rotated directional coupler is *four* port *two* direction device, the transfer matrix for rotated directional coupler can be derived by comparison and calculation of (4.12) and (4.30). So the transfer matrix for rotated directional coupler can be written as:

$$T = \frac{1}{j\sqrt{\epsilon}} \begin{bmatrix} -1 & \sqrt{1-\epsilon} \\ -\sqrt{1-\epsilon} & 1 \end{bmatrix}. \tag{4.31}$$

4.2.4 Transmittivity and Phase Transfer Functions

Transmission Coefficient τ_{13}

Transmission coefficient τ_{13} for *four* port *two* direction device is derived in 4.1.3. From (4.20), transmission coefficient τ_{13} for rotated directional coupler can be written as:

$$\tau_{13} = -\frac{C}{D}.$$

Comparing (4.5) and (4.30), calculate value of C and D. Substituting this value in the above equation gives τ_{13} for rotated directional coupler.

$$\tau_{13} = \sqrt{1-\epsilon}. \tag{4.32}$$

So transmission coefficient τ_{13} of a rotated directional coupler is $\sqrt{1-\epsilon}$.

Transmission Coefficient τ_{14}

Transmission coefficient τ_{14} for *four* port *two* direction device is derived in 4.1.3. From (4.24), transmission coefficient τ_{14} for rotated directional coupler can be written as:

$$\tau_{14} = \frac{AD - BC}{D}.$$

Comparing (4.5) and (4.30), calculate value of A, B, C and D. Substituting this value in the above equation gives τ_{14} for rotated directional coupler.

$$\tau_{14} = j\sqrt{\epsilon}. \tag{4.33}$$

So transmission coefficient τ_{14} of a rotated directional coupler is $j\sqrt{\epsilon}$.

Transmittivitty T_{13}

As the transmittivity T_{13} is the fraction of power transmitted from the input port P1 to the output port P3 passing through coupling region of a rotated directional coupler, it is calculated from transmission coefficient τ_{13} as follows:

$$\begin{aligned}
T_{13} &= |\tau_{13}|^2, \\
T_{13} &= \tau_{13} * \tau_{13}^*, \\
T_{13} &= \sqrt{1-\epsilon} * (\sqrt{1-\epsilon^*})^*, \\
T_{13} &= \sqrt{1-\epsilon} * \sqrt{1-\epsilon^*}, \\
T_{13} &= (1-\epsilon).
\end{aligned} \tag{4.34}$$

So the transmittivity T_{13} of a directional coupler is $(1-\epsilon)$.

Transmittivitty T_{14}

As the transmittivity T_{14} is the fraction of power transmitted from the input port P1 to the output port P4 passing through coupling region of a rotated directional coupler, it is calculated from transmission coefficient τ_{14} as follows:

$$\begin{aligned} T_{14} &= |\tau_{14}|^2, \\ T_{14} &= \tau_{14} * \tau_{14}^*, \\ T_{14} &= j\sqrt{\epsilon} * (j\sqrt{\epsilon})^*, \\ T_{14} &= j\sqrt{\epsilon} * (-j\sqrt{\epsilon}), \\ T_{14} &= \epsilon. \end{aligned} \tag{4.35}$$

So the transmittivity T_{13} of a directional coupler is ϵ.

Transmittivity vs. ϵ Spectra

As seen in (4.34) and (4.35), the transmittivity of rotated directional coupler is dependent upon ϵ. The graph in Fig. 4.3 shows how the transmittivity T_{13} and T_{14} varies with ϵ. As seen in Fig. 4.3, T_{13} decreases as ϵ increases whereas T_{14} increases with ϵ.

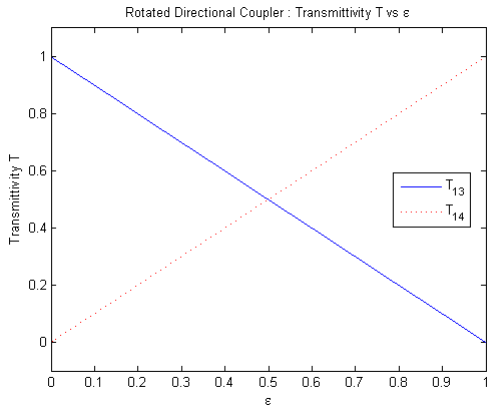

Figure 4.3: Transmittivity vs. ϵ

Phase Transfer Function ϕ_{13}

As phase transfer functions ϕ_{13} is the phase difference between the input at port P1 to the output at port P3 after passing through coupling region of coupler, it is calculated from transmission coefficient τ_{13} as follows:

$$\begin{aligned}
&\phi_{13} = arg(\tau_{13}),\\
&\phi_{13} = arg(\sqrt{1-\epsilon}),\\
&\phi_{13} = tan^{-1}\left(\frac{0}{\sqrt{1-\epsilon}}\right),\\
&\phi_{13} = 0.
\end{aligned} \tag{4.36}$$

So phase transfer functions ϕ_{13} of a rotated directional coupler is 0.

Phase Transfer Function ϕ_{14}

As phase transfer functions ϕ_{14} is the phase difference between the input at port P1 to the output at port P4 after passing through coupling region of coupler, it is calculated from transmission coefficient τ_{14} as follows:

$$\phi_{14} = arg(\tau_{14}),$$

$$\phi_{14} = arg(j\sqrt{\epsilon}),$$

$$\phi_{14} = tan^{-1}\left(\frac{\sqrt{\epsilon}}{0}\right), \tag{4.37}$$

$$\phi_{14} = \frac{\pi}{2}. \tag{4.38}$$

So phase transfer functions ϕ_{14} of a rotated directional coupler is $\frac{\pi}{2}$.

Phase Transfer Function vs. ϵ Spectra

As seen in (4.36) and (4.38), phase transfer function of directional coupler is not dependent upon ϵ. The graph in Fig. 4.4 shows that even ϵ changes, phase transfer functions ϕ_{13} and ϕ_{14} remains same. As seen in Fig. 4.4, ϕ_{13} is 0 and ϕ_{14} is $\frac{\pi}{2}$ for all values of ϵ.

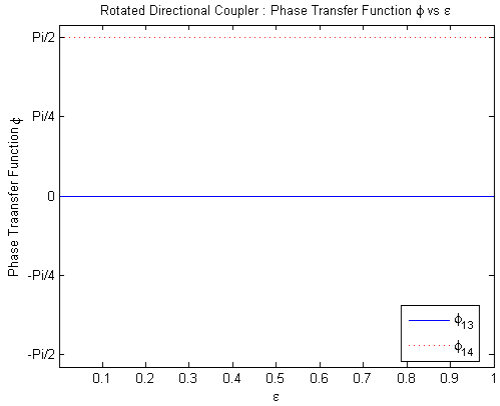

Figure 4.4: Phase Transfer Function vs. ϵ

4.2.5 Conservation of Power

As mentioned in chapter 3, for conservation of power, total of all the transmittivity and the reflectivity of a device must be equal to 1.

The above in rotated directional coupler, we considered the input only at port P1 and we considered the input at port P2 as 0. So power from port P1 is transmitted to only port P3 and port P4 as as there is no coupling between the input port P1 to port P2 and there is no reflection at port P1. As stated the above, for conservation of a power in lossless rotated directional coupler, total of the transmittivity T_{13} and transmittivity T_{14} must be 1.

$$\begin{aligned} T_{Total} &= T_{13} + T_{14}, \\ T_{Total} &= 1 - \epsilon + \epsilon, \\ T_{Total} &= 1. \end{aligned} \tag{4.39}$$

As total transmittivity is equal to 1, there is conservation of power in lossless rotated directional coupler.

4.2.6 Unitaryness of a Transfer Matrix

A square matrix U is unitary if

$$U^H = U^{-1}. \tag{4.40}$$

where U^H denotes the conjugate transpose and U^{-1} is the matrix inverse.

So to verify that the transfer matrix for directional coupler with unidirectional waveguide is unitary matrix, calculate conjugate transpose and matrix inverse of the transfer matrix. Conjugate transpose is as below:

$$T^H = \frac{j}{\sqrt{\epsilon}} \begin{bmatrix} -1 & -\sqrt{1-\epsilon} \\ \sqrt{1-\epsilon} & 1 \end{bmatrix}. \tag{4.41}$$

Also inverse of the transfer matrix is given as below:

$$T^{-1} = \frac{j}{\sqrt{\epsilon}} \begin{bmatrix} -1 & \sqrt{1-\epsilon} \\ -\sqrt{1-\epsilon} & 1 \end{bmatrix}. \tag{4.42}$$

Comparing (4.41) and (4.42), we get that

$$T^H \neq T^{-1}. \tag{4.43}$$

So the transfer matrix of directional coupler with unidirectional waveguide is not unitary matrix.

4.2.7 Determinant of a Transfer Matrix

Determinant of the transfer matrix of rotated directional coupler with unidirectional waveguides is given as below:

$$\begin{aligned} det(T) &= \frac{1}{j\sqrt{\epsilon}} \begin{vmatrix} -1 & \sqrt{1-\epsilon} \\ -\sqrt{1-\epsilon} & 1 \end{vmatrix}, \\ det(T) &= 1. \end{aligned} \tag{4.44}$$

So determinant of a symmetric lossless rotated directional coupler with unidirectional waveguide is 1.

4.3 Rotated Directional Coupler with Ghost Waveguide

4.3.1 Introduction

Ghost Waveguide

One of several meaning of *ghost* is a faint trace of something. So similarly ghost waveguide is waveguide which is fabricated for the purpose of convenience but with a a faint trace of it in a device . Ghost waveguides concept used in the thesis is for the purpose of the modeling photonic loop structures. For convenience of calculation and derivations, for some devices we considered presence of ghost waveguides but these waveguides are not present in device. The ghost waveguide concept used is applied and verified for rotated directional coupler in next section.

Rotated Directional Coupler with Ghost Waveguide

Rotated directional coupler with ghost waveguide is as shown in Fig. 4.3. As seen in figure, rotated directional coupler with ghost waveguide is same as rotated directional coupler but one of the waveguide is ghost waveguide. So we will consider the existence of a ghost waveguide until needed. When ghost waveguide is not required, we will consider coupling between waveguides as 0.

As shown in Fig. 4.5, rotated directional coupler comprises of four ports P1, P2, P3 and P4. Port P1 and port P3 are of real waveguide and port P2 and P4 are of ghost waveguide. Ports P1 and P2 acts as the input port and ports P3 and P4 acts as the output port. E_1^+ and E_2^- denotes the input field strengths of port P1 and P2. So forget the concept of ghost waveguide for now. So Fig. 4.5 is same as rotated directional coupler in Fig. 4.2. So transmission parameters for rotated directional coupler with ghost waveguide is same as rotated directional coupler.

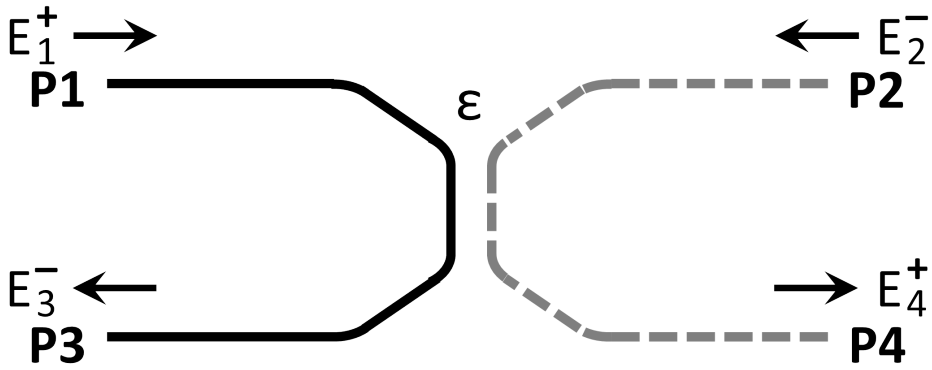

Figure 4.5: Rotated Directional Coupler with Ghost Waveguide

4.3.2 Transmittivity and Phase Transfer Functions

Transmittivitty T_{13}

As transmission parameters for rotated directional coupler with ghost waveguide is same as rotated directional coupler, the transmittivity T_{13} for rotated directional coupler with ghost waveguide is same as rotated directional coupler. So from (4.34), the transmittivity T_{13} can be written as:

$$T_{13} = (1 - \epsilon). \tag{4.45}$$

Now, consider the existence of ghost waveguide. So as ghost waveguide is not really present, it is fabricated for convenience of calculation. So to neglect existence of ghost waveguide consider the coupling coefficient as 0 i.e. $\epsilon = 0$. So there is no coupling between real waveguide and ghost waveguide resulting in no power transfer. So ghost waveguide is not present. So the transmittivity T_{13} of a rotated directional coupler with ghost waveguide is $(1 - 0)$. i.e. 1

Phase Transfer Function ϕ_{13}

As transmission parameters for rotated directional coupler with ghost waveguide is same as rotated directional coupler, the phase transfer function ϕ_{13} for rotated directional coupler

with ghost waveguide is same as rotated directional coupler. So from (4.36), the transmittivity T_{13} rotated directional coupler with ghost waveguide is 0.

Transmittivitty T_{14}

As transmission parameters for rotated directional coupler with ghost waveguide is same as rotated directional coupler, the transmittivity T_{14} for rotated directional coupler with ghost waveguide is same as rotated directional coupler. So from (4.35), the transmittivity T_{14} can be written as:

$$T_{14} = \epsilon. \tag{4.46}$$

As stated the above, to neglect existence of ghost waveguide consider the coupling coefficient as 0 i.e. $\epsilon = 0$. So the transmittivity T_{14} of a rotated directional coupler with ghost waveguide is 0. This proves that there is no transfer of power from port P1 to port P4.

Phase Transfer Function ϕ_{14}

As transmission parameters for rotated directional coupler with ghost waveguide is same as rotated directional coupler, the phase transfer function ϕ_{14} for rotated directional coupler with ghost waveguide is same as rotated directional coupler. So from (4.37), the transmittivity T_{14} rotated directional coupler with ghost waveguide is 0.

4.3.3 Conservation of Power

As mentioned in chapter 2, for conservation of power, total of all transmittivity and the reflectivity of a device must be equal to 1.

The above in rotated directional coupler with ghost waveguide, we considered the input only at port P1 and we considered the input at port P2 as (same as rotated directional coupler). As stated the above, for conservation of a power in lossless rotated directional

coupler with ghost waveguide, total of the transmittivity T_{13} and transmittivity T_{14} must be 1.

$$T_{Total} = T_{13} + T_{14},$$
$$T_{Total} = 1. \tag{4.47}$$

As total transmittivity is equal to 1, there is conservation of power in lossless rotated directional coupler with ghost waveguide. The ghost waveguide is not affecting the transfer of power.

Chapter 5

Parallel Waveguides

5.1 Four Port Bidirectional Device

Four-port bidirectional device contains four ports (two input and two output ports) and device is bidirectional in nature. This device is similar to four-port bidirectional device in 4.1 but difference between these two devices is direction of the light streams traveling in ports. As shown in Fig. 5.1, four port bidirectional device comprises of two input ports P1 and P4 and two output ports P2 and P3, and light traveling in device is in left to right direction at ports P1 and P2 and in right to left direction at port P3 and P4. But in as shown in Fig. 4.1, four port unidirectional devices comprises of two input ports P1 and P2 and two output ports P3 and P4, and light traveling in device is in left to right direction at ports P1 and P4 and in right to left direction at port P2 and P3.

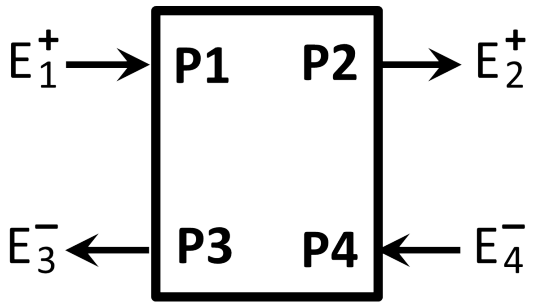

Figure 5.1: Four-Port Bidirectional Device

E_1^+ ans E_4^- denotes the input field strengths of port P1 and P4 whereas E_2^+ and E_3^- denotes the output field strengths of port P2 and P3. The total input in the device is denoted

by *a* and the total output in the device is denoted by *b*. So input *a* and output *b* for Fig. 5.1 can be represented in matrix form as below:

$$a = \begin{bmatrix} E_1^+ \\ E_4^- \end{bmatrix}, \tag{5.1}$$

$$b = \begin{bmatrix} E_2^+ \\ E_3^- \end{bmatrix}. \tag{5.2}$$

5.1.1 Scattering Matrix

As mentioned in 3.1.1, scattering matrix correlates the coefficients of the input state of a photonic device or system to the coefficients of the output state of a photonic device or system. So from (3.3), scattering matrix *S* which correlates the coupling of optical power transfer from input *a* to output *b* is given as,

$$b = Sa. \tag{5.3}$$

The correlation between input *a* in 5.1 and output *b* in 5.2 along with scattering matrix *S* for the *four* port *two* directional device in Fig. 5.1 is given as,

$$\begin{bmatrix} E_2^+ \\ E_3^- \end{bmatrix} = \begin{bmatrix} s_{12} & s_{42} \\ s_{13} & s_{43} \end{bmatrix} \begin{bmatrix} E_1^+ \\ E_4^- \end{bmatrix}. \tag{5.4}$$

5.1.2 Formation of Transfer Matrix

Transfer Matrix

As mentioned in 3.1.2, *transfer matrix* correlates the coefficients of states on the left side of the coupling region to the coefficients of states on the right side of the coupling region. So the transfer matrix *T* for the *four* port *two* direction device in Fig. 5.1 is given as,

$$T = \begin{bmatrix} A & B \\ C & D \end{bmatrix}. \tag{5.5}$$

The correlation between the coefficients of states on the left side of the coupling region and the coefficients of states on the right side of the coupling region along with transfer matrix *T* for the *four* port *two* direction device in Fig. 5.1 is given as,

$$\begin{bmatrix} E_2^+ \\ E_4^- \end{bmatrix} = \begin{bmatrix} A & B \\ C & D \end{bmatrix} \begin{bmatrix} E_1^+ \\ E_3^- \end{bmatrix}. \tag{5.6}$$

Formation of Transfer matrix

As stated in chapter 3, in analysis and calculations transfer parameters of a device, transfer matrices are more appropriate than scattering matrices. So scattering matrix can be derived initially and with the help of scattering matrix, transfer matrix can be derived. So in this section, matrix formula for formation of transfer matrix from scattering matrix is derived.

From Fig. 5.1 and (5.6), it can be observed that one input and one output is on either side of a coupling region. So for formation of transfer matrix from scattering matrix, it is obligatory to expand and rearrange the scattering matrix in 5.4. By expansion of 5.4, we get following equations,

$$E_2^+ = s_{12}E_1^+ + s_{42}E_4^-, \tag{5.7}$$

$$E_3^- = s_{13}E_1^+ + s_{43}E_4^-. \tag{5.8}$$

Rearranging (5.8), we get

$$\begin{aligned} E_3^- &= s_{13}E_1^+ + s_{43}E_4^-, \\ E_4^- &= -\frac{s_{13}}{s_{43}}E_1^+ + \frac{1}{s_{43}}E_3^-. \end{aligned} \tag{5.9}$$

Substitute value of E_4^- in (5.7),

$$\begin{aligned} E_2^+ &= s_{12}E_1^+ + s_{42}\left[-\frac{s_{13}}{s_{43}}E_1^+ + \frac{1}{s_{43}}E_3^-\right], \\ E_2^+ &= s_{12}E_1^+ - \frac{s_{13}s_{42}}{s_{43}}E_1^+ + \frac{s_{42}}{s_{43}}E_3^-, \\ E_2^+ &= \frac{s_{12}s_{43} - s_{13}s_{42}}{s_{43}}E_1^+ + \frac{s_{42}}{s_{43}}E_3^-. \end{aligned} \tag{5.10}$$

By arranging (5.9) and (5.10) in matrix form, we get

$$\begin{bmatrix} E_2^+ \\ E_4^- \end{bmatrix} = \frac{1}{s_{43}} \begin{bmatrix} s_{12}s_{43} - s_{13}s_{42} & s_{42} \\ -s_{13} & 1 \end{bmatrix} \begin{bmatrix} E_1^+ \\ E_3^- \end{bmatrix}, \tag{5.11}$$

The (5.11) is similar to (5.6). So *transfer matrix* for *four* port *two* direction device in Fig. 5.1 is written as,,

$$T = \frac{1}{s_{43}} \begin{bmatrix} s_{12}s_{43} - s_{13}s_{42} & s_{42} \\ -s_{13} & 1 \end{bmatrix}, \tag{5.12}$$

5.1.3 Transmission Parameters

As mentioned in previous chapter, transmission parameters provides some information about transmission of power in device. By expansion of (5.6), we get following equations,

$$E_2^+ = AE_1^+ + BE_3^-, \tag{5.13}$$

$$E_4^- = CE_1^+ + DE_3^-. \tag{5.14}$$

If light E_1^+ is launched at port P1 and input at port P4 is 0 , then substituting $E_4^- = 0$ in above equations gives following equations:

$$E_2^+ = AE_1^+ + BE_3^-, \tag{5.15}$$

$$0 = CE_1^+ + DE_3^-. \tag{5.16}$$

Transmission coefficient τ_{13}

Transmission coefficient τ_{13} can be written as,

$$\tau_{13} = \frac{E_3^-}{E_1^+}. \tag{5.17}$$

Restructuring (5.16), we get following equation:

$$\begin{aligned} DE_3^- &= -CE_1^+, \\ E_3^- &= -\frac{C}{D}E_1^+, \qquad (5.18) \\ \frac{E_3^-}{E_1^+} &= -\frac{C}{D}, \qquad (5.19) \\ \tau_{13} &= -\frac{C}{D}. \qquad (5.20) \end{aligned}$$

So transmission coefficient τ_{13} can be given as $-\frac{C}{D}$.

Transmission Coefficient τ_{12}

Transmission coefficient τ_{14} can be written as,

$$\tau_{12} = \frac{E_2^+}{E_1^+}. \tag{5.21}$$

Substitute value of E_3^- from (5.18) into (5.15), we get following equation:

$$\begin{aligned} E_2^+ &= AE_1^+ + B\left[-\frac{C}{D}E_1^+\right], \\ E_2^+ &= AE_1^+ - \frac{BC}{D}E_1^+. \\ E_2^+ &= \frac{AD-BC}{D}E_1^+, \qquad (5.22) \\ \frac{E_2^+}{E_1^+} &= \frac{AD-BC}{D}, \qquad (5.23) \\ \tau_{12} &= \frac{AD-BC}{D}. \qquad (5.24) \end{aligned}$$

So transmission coefficient τ_{12} can be given as $\frac{AD-BC}{D}$.

5.2 Parallel Waveguides

5.2.1 Introduction

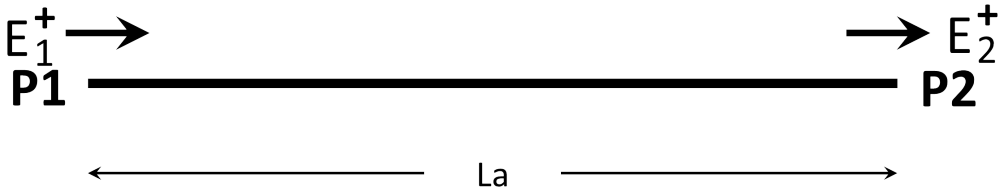

Figure 5.2: Unidirectional Waveguide

Unidirectional Waveguide As described in 1.3.1, photonic waveguide shown in Fig. 5.2 is is simple component with two ports P1 and P2. Port P1 is an input port and port P2 is an output port. Field strength at port P1 and port P2 is denoted as E_1^+ and E_2^+. The relation between input E_1^+ and output E_2^+ can be given as,

$$E_2^+ = e^{(-\frac{\alpha}{2}+i\beta)L} E_1^+. \tag{5.25}$$

where, α and $\beta(= 2\pi n/\lambda)$ represent the fiber attenuation and propagation constants, respectively and L is the length of a waveguide. The above equation is equivalent to equation (2.3.2) in [1].

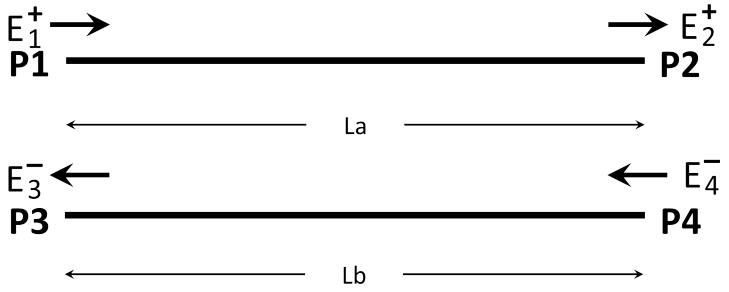

Figure 5.3: Parallel Unidirectional Waveguide

Parallel Waveguide As shown in fig 5.3 ,2 unidirectional waveguides are parallel to each other and light stream is traveling from left to right in one waveguide and right to left in another waveguide. As direction of light stream does not affect the field strength in a waveguide, the relation between field strength at input and field strength at output for waveguide of length L is given as,

$$E_{output} = e^{(-\frac{\alpha}{2}+i\beta)L} E_{input}. \tag{5.26}$$

In Fig. 5.3, there are two input ports P1 and P4 and two output ports P2 and P3. Field strength at port P1, P2, P3 and P4 is denoted as E_1^+, E_2^+, E_3^- and E_4^- respectively. So input *a* and output *b* for Fig. 5.3 is given as,

$$a = \begin{bmatrix} E_1^+ \\ E_4^- \end{bmatrix}, \tag{5.27}$$

$$b = \begin{bmatrix} E_2^+ \\ E_3^- \end{bmatrix}. \tag{5.28}$$

5.2.2 Scattering Matrix

As mentioned in 3.1.1, scattering matrix correlates the coefficients of the input state of a photonic device or system to the coefficients of the output state of a photonic device or system. So from (3.3), scattering matrix *S* which correlates the coupling of optical power transfer from input *a* to output *b* is given as,

$$b = Sa, \tag{5.29}$$

From (5.26), (5.27) and (5.28), correlation between input, output and scattering matrix S for the directional coupler in Fig. 5.2 is given as,

$$\begin{bmatrix} E_2^+ \\ E_3^- \end{bmatrix} = \begin{bmatrix} s_{12} & s_{42} \\ s_{13} & s_{43} \end{bmatrix} \begin{bmatrix} E_1^+ \\ E_4^- \end{bmatrix}. \tag{5.30}$$

As two waveguides are parallel to each other there is no coupling between them. So there is no coupling from port P1 to port P3 and from port P4 to port P2. This leads to $s_{13} = 0$ and $s_{42} = 0$. Substituting these values in above equation, we get

$$\begin{bmatrix} E_2^+ \\ E_3^- \end{bmatrix} = \begin{bmatrix} s_{12} & 0 \\ 0 & s_{43} \end{bmatrix} \begin{bmatrix} E_1^+ \\ E_4^- \end{bmatrix}. \tag{5.31}$$

s_{12} represents transfer of power from port P1 to port P2 for waveguide of length of La and s_{43} represents transfer of power from port P4 to port P3 for waveguide of length Lb. As (5.26) represents the relation between input and output of photonic waveguide, s_{12} and s_{43} can be written as,

$$s_{12} = e^{(-\frac{\alpha}{2}+i\beta)La}, \tag{5.32}$$

$$s_{43} = e^{(-\frac{\alpha}{2}+i\beta)Lb}. \tag{5.33}$$

Substituting these values in (5.30), we get following equation

$$\begin{bmatrix} E_2^+ \\ E_3^- \end{bmatrix} = \begin{bmatrix} e^{(-\frac{\alpha}{2}+i\beta)La} & 0 \\ 0 & e^{(-\frac{\alpha}{2}+i\beta)Lb} \end{bmatrix} \begin{bmatrix} E_1^+ \\ E_4^- \end{bmatrix}. \tag{5.34}$$

So scattering matrix of parallel waveguides can be written as,

$$S = \begin{bmatrix} e^{(-\frac{\alpha}{2}+i\beta)La} & 0 \\ 0 & e^{(-\frac{\alpha}{2}+i\beta)Lb} \end{bmatrix}. \tag{5.35}$$

5.2.3 Formation of Transfer Matrix

Transfer matrix for *four* port *two* direction device is derived in 5.1.2. (5.12) provides a formula to derive the transfer matrix from scattering matrix for *four* port *two* direction device. As parallel waveguide is *four* port *two* direction device, transfer matrix for rotated directional coupler can be derived by comparison and calculation of (5.12) and (5.35). So transfer matrix for rotated directional coupler can be written as:

$$T = \begin{bmatrix} e^{(-\frac{\alpha}{2}+i\beta)La} & 0 \\ 0 & e^{(\frac{\alpha}{2}-i\beta)Lb} \end{bmatrix}. \tag{5.36}$$

So the transfer matrix parameters mentioned above for parallel unidirectional waveguides are equivalent to transfer matrix parameters for pair of fibers mentioned in [12] and single-mode fiber channel in [2]. They are not same as the transfer matrix concept used in [12] and [2] and concept we used is not same. In [12] and [2], coefficients of states on the right side of the coupling region are multiplied by transfer matrix of a photonic device to get the coefficients of states on the left side of the coupling region. Opposite to this, in our derivation, coefficients of states on the left side of the coupling region are multiplied by transfer matrix of a photonic device to get the coefficients of states on the right side of the coupling region.

5.2.4 Transmittivity and Phase Transfer Functions

Transmission Coefficient τ_{12}

Transmission coefficient τ_{12} for *four* port *two* direction device is derived in 5.1.3. From (5.24), transmission coefficient τ_{12} for parallel waveguides can be written as:

$$\tau_{12} = \frac{AD - BC}{D}.$$

Comparing (5.5) and (5.36), calculate value of A, B, C and D. Substituting this value in above equation gives τ_{12} for parallel waveguides.

$$\tau_{12} = e^{(-\frac{\alpha}{2}+i\beta)La}. \tag{5.37}$$

So transmission coefficient τ_{12} of a parallel waveguides is $e^{(-\frac{\alpha}{2}+i\beta)La}$.

Transmission Coefficient τ_{13}

Transmission coefficient τ_{13} for *four* port *two* direction device is derived in 5.1.3. From (5.20), transmission coefficient τ_{13} for parallel waveguides can be written as:

$$\tau_{13} = -\frac{C}{D}.$$

Comparing (5.5) and (5.36), calculate value of C and D. Substituting this value in above equation gives τ_{13} for parallel waveguides.

$$\tau_{13} = 0. \tag{5.38}$$

So transmission coefficient τ_{13} of parallel waveguides is 0.

Transmittivity T_{12}

As transmittivity T_{12} is fraction of power transmitted from input port P1 to the output port P2 , it is calculated from transmission coefficient τ_{12} as follow:

$$\begin{aligned} T_{12} &= |\tau_{12}|^2, \\ T_{12} &= \tau_{12} * \tau_{12}^*, \\ T_{12} &= e^{(-\frac{\alpha}{2}+i\beta)La} * (e^{(-\frac{\alpha}{2}+i\beta)La})^*, \\ T_{12} &= e^{(-\alpha La)}. \end{aligned} \tag{5.39}$$

So transmittivity T_{12} of a parallel waveguide is $e^{(-\alpha La)}$.

Transmittivitty T_{13}

As transmittivity T_{13} is fraction of power transmitted from input port P1 to the output port P3 , it is calculated from transmission coefficient τ_{13} as follow:

$$\begin{aligned} T_{13} &= |\tau_{13}|^2, \\ T_{13} &= \tau_{13} * \tau_{13}^*, \\ T_{13} &= 0. \end{aligned} \tag{5.40}$$

So transmittivity T_{13} of a parallel waveguides is 0.

Transmittivity vs. $\frac{\beta L}{\pi}$ Spectra

As seen above, the transmittivity of the parallel waveguides is dependent upon α and, β and L. The graph in Fig. 5.4 and Fig. 5.5 shows how the transmittivity T_{12} and T_{12} varies with $\frac{\beta L}{\pi}$ respectively. As seen in Fig. 5.4, T_{12} remains 1 as ϵ increases whereas T_{14} remains 0.

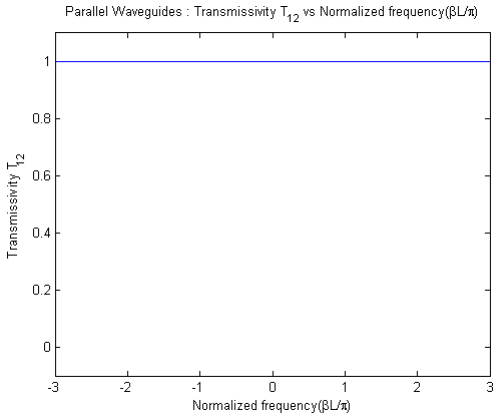

Figure 5.4: Transmittivity T_{12} vs. $\frac{\beta L}{\pi}$

Phase Transfer Function ϕ_{12}

As phase transfer functions ϕ_{12} is the phase difference between the input at port P1 to the output at port P2 , it is calculated from transmission coefficient τ_{12} as follow:

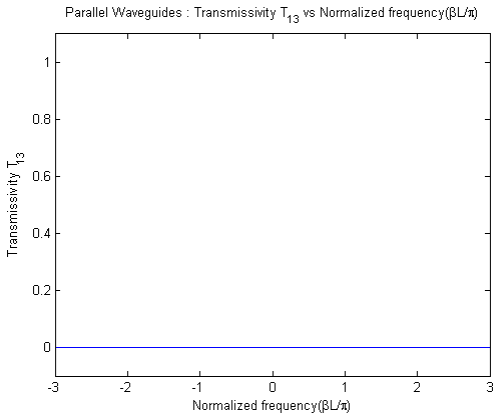

Figure 5.5: Transmittivity T_{13} vs. $\frac{\beta L}{\pi}$

$$\begin{aligned}
\phi_{12} &= arg(\tau_{12}), \\
\phi_{12} &= arg(e^{(-\frac{\alpha}{2}+i\beta)La}, \\
\phi_{12} &= \frac{\pi}{2}.
\end{aligned} \tag{5.41}$$

So phase transfer functions ϕ_{10} of parallel waveguides is $\frac{\pi}{2}$.

Phase Transfer Function ϕ_{13}

As phase transfer functions ϕ_{13} is the phase difference between the input at port P1 to the output at port P3 , it is calculated from transmission coefficient τ_{13} as follow:

$$\begin{aligned}
\phi_{13} &= arg(\tau_{13}), \\
\phi_{13} &= arg(0), \\
\phi_{13} &= tan^{-1}(0), \\
\phi_{13} &= 0.
\end{aligned} \tag{5.42}$$

So phase transfer functions ϕ_{13} of a parallel waveguides is 0.

Phase Transfer Function vs. ϵ Spectra

As seen in above equations, the phase transfer function the parallel waveguides is not dependent upon α or β. The graph in Fig. 5.8 and Fig. 5.9 shows that how ϕ_{12} changes with the change in βL, whereas ϕ_{14} remains same 0 .

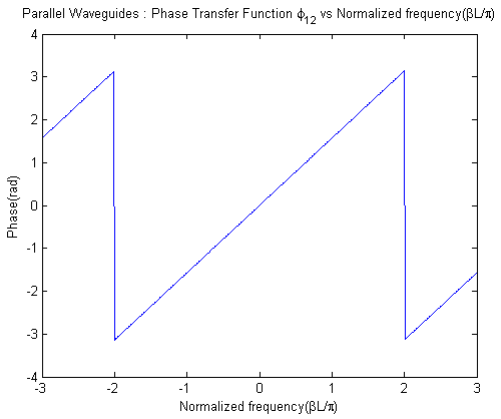

Figure 5.6: Phase Transfer Function ϕ_{12} vs. $\frac{\beta L}{\pi}$

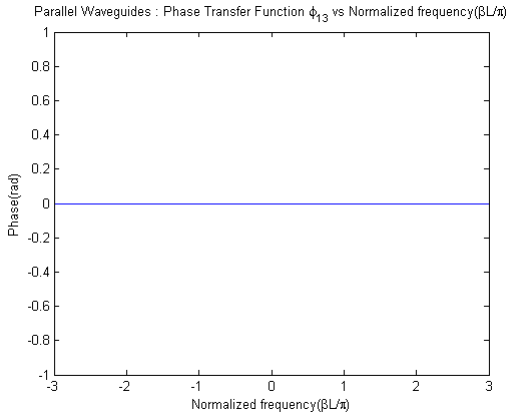

Figure 5.7: Phase Transfer Function ϕ_{13} vs. $\frac{\beta L}{\pi}$

5.2.5 Conservation of Power

As mentioned in chapter 3, for conservation of power, total of all transmittivity and reflectivity of a device must be equal to 1.

Above in parallel waveguides, we considered input only at port P1 and we considered input at port P4 as 0. So power from port P1 is transmitted to only port P2 as as there is no coupling between two waveguides and there is no reflection at port P1. Also for parallel waveguides to be lossless, fiber attenuation α must be 0. As stated above, for conservation of a power in lossless rotated directional coupler, total of transmittivity T_{13} and transmittivity T_{14} must be 1.

$$\begin{aligned} T_{Total} &= T_{12} + T_{13}, \\ T_{Total} &= e^{(-\alpha La)}, \\ T_{Total} &= 1. \end{aligned} \tag{5.43}$$

As total transmittivity is equal to 1, there is conservation of power in lossless parallel waveguides.

5.2.6 Unitaryness of a Transfer Matrix

To check that transfer matrix for parallel unidirectional waveguide is unitary matrix, consider that device is lossless device. As α is fiber attenuation, consider it as 0 to change device to lossless device. So transfer matrix of parallel unidirectional waveguide for lossless device is written as :

$$T = \begin{bmatrix} e^{(i\beta)La} & 0 \\ 0 & e^{(-i\beta)Lb} \end{bmatrix}. \tag{5.44}$$

So to verify that transfer matrix for parallel unidirectional waveguide is unitary matrix, calculate conjugate transpose and matrix inverse of transfer matrix. Calculate conjugate transpose and matrix inverse of transfer matrix for lossless case. Conjugate transpose is as below:

$$T^H = \begin{bmatrix} e^{(-i\beta)La} & 0 \\ 0 & e^{(i\beta)Lb} \end{bmatrix}. \tag{5.45}$$

Also inverse of transfer matrix is given as below:

$$T^{-1} = \begin{bmatrix} e^{(-i\beta)La} & 0 \\ 0 & e^{(i\beta)Lb} \end{bmatrix}. \tag{5.46}$$

Comparing (3.52) and (3.53), we get that

$$T^H = T^{-1}. \tag{5.47}$$

So transfer matrix of parallel unidirectional waveguide is unitary matrix.

5.2.7 Determinant of a Transfer Matrix

To derive the determinant of a parallel unidirectional device consider length of both waveguides equal i.e. $La = Lb = L$ .Determinant of transfer matrix of parallel unidirectional waveguides is given as below:

$$\begin{aligned} det(T) &= \begin{vmatrix} e^{(-\frac{\alpha}{2}+i\beta)L} & 0 \\ 0 & e^{(\frac{\alpha}{2}-i\beta)L} \end{vmatrix}, \\ det(T) &= 1. \end{aligned} \tag{5.48}$$

So determinant of a parallel unidirectional waveguides is 1.

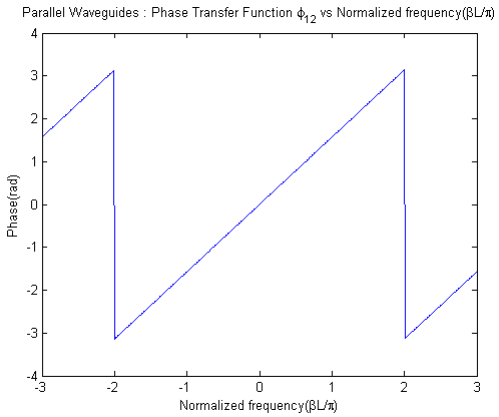

Figure 5.8: Phase Transfer Function ϕ_{12} vs. $\frac{\beta L}{\pi}$

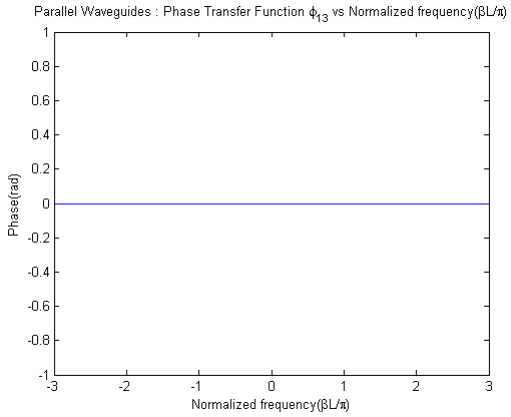

Figure 5.9: Phase Transfer Function ϕ_{13} vs. $\frac{\beta L}{\pi}$

Chapter 6

Dual-Waveguide Ring Resonator

6.1 Introduction

6.1.1 Dual-Waveguide Ring Resonator

A a dual-waveguide ring resonator can be designed, as shown in Fig. 6.1, by placing the photonic-ring between two parallel photonic waveguides. This device is also called as the two-coupler ring resonator as the ring is coupled to two parallel waveguides.

As seen in Fig. 6.1, there are four ports in the device. When the light is entered in the input port as seen in Fig. 6.1,it travels towards the coupling region with the coupling coefficient ϵ_1. When it reaches the coupling region with the coupling coefficient ϵ_1, some quantity of power from the input port is coupled into the ring and the remaining power in dissipated at the throughput port. The power coupled into the ring travels in the ring till it reaches the second coupling region with the coupling coefficient ϵ_2. At this point also some quantity of power from the ring is coupled into the drop port and the remaining power is re-transmitted into the ring. The power re-transmitted in the ring travels in the ring till the coupling region 1. At this point it again combines with power from the input port and some of power is coupled to throughput region whereas some of it is re-transmitted into the ring. So some quantity of power keeps circulating in the ring.

6.1.2 Concatenated Structures

Sometimes, some basic structures are used to form complex structures. So concatenated structures are such complex structures in which basic structures are connected to each other

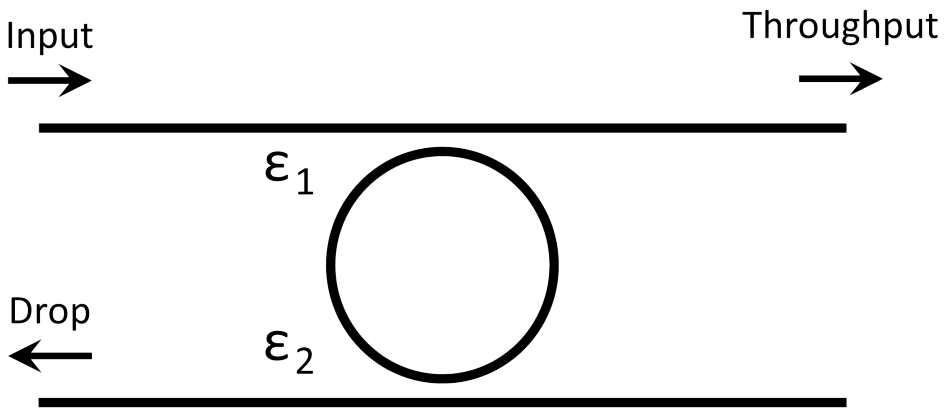

Figure 6.1: Dual-Waveguide Ring Resonator

after one another by waveguides. As shown in Fig. 6.2, three photonic structures Z1 and Z2 are connected to each other by waveguides and structure Z2 is connected to another structure Z3 by waveguides. This is called concatenations of structure. This can be a long chain of structures concatenated to each other.

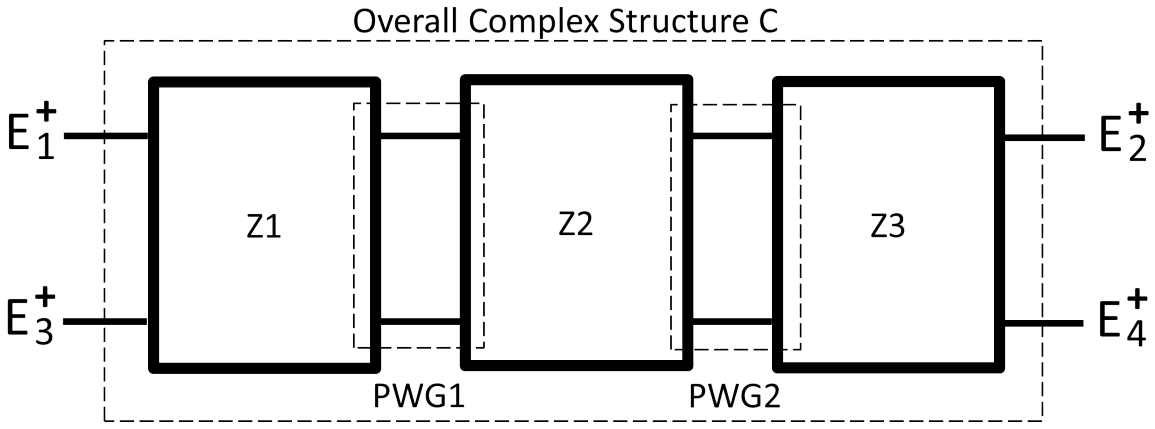

Figure 6.2: Concatenated Structures

As this chain of structures concatenated structures increases, it is really difficult to to model these structure using method of equating field or method of unfolded equivalent system. On contrary it is quite simple to model these complex photonic structures if transfer matrices of basic structures Z1, Z2 and Z3. Consider field strength at 4 ports are given by E_1^+, E_2^+, E_3^+ and E_4^+. So the transfer matrix of complex structure T_C in Fig. 6.2 is given

as

$$\begin{bmatrix} E_2^+ \\ E_4^+ \end{bmatrix} = T_C \begin{bmatrix} E_1^+ \\ E_3^+ \end{bmatrix}.$$

Assume that transfer matrices of these basic structures are represented by T_{Z1},T_{Z2}, T_{Z3} respectively and the transfer matrix of parallel waveguides connected these basic structures is represented by T_{PWG1} and T_{PWG2}. Transfer matrix of a complex structure is represented by T_C. So the transfer matrix of a complex structure T_C is calculated by matrix multiplication of the transfer matrix of basic structures and parallel waveguides from right to left order. So the transfer matrix of a complex structure T_C is calculated as

$$T_C = [T_{Z3}][T_{PWG2}][T_{Z2}][T_{PWG1}][T_{Z1}].$$

6.1.3 Dual-Waveguide Ring Resonator as Concatenated Structure

From Fig. 6.1, it can be observed that a dual-waveguide ring resonator has two coupling regions with coupling coefficients ϵ_1 and ϵ_2. These two coupling regions forms two directional couplers. Rotating Fig. 6.1 90^o anticlockwise and splitting it, we get Fig. 6.3. From Fig. 6.3, it can be observed that, a dual-waveguide ring resonator is obtained by a concatenation of the rotated directional coupler, parallel waveguides and finally another the rotated directional coupler. As there are two rotated directional couplers, we call the rotated directional coupler on left as *RDC1* and the rotated directional coupler on right is called as *RDC2*.Lets call the parallel waveguides as *PWG*.

As seen in Fig. 6.3, RDC1 has four ports P1, P3, $P2^{'}$ and $P4^{'}$. Similarly, ports for RDC2 are designated as P2, P4, $P1^{'}$ and $P4^{'}$. But for overall coupled structure i.e. a dual-waveguide ring resonator, the four ports are P1, P2, P3 and P4. Field strength at P1, P2, P3 and P4 is given by E_1^-, E_2^-, E_3^+ and E_4^+ respectively. For a dual-waveguide ring resonator, port P3 and P2 acts as the input port and port P1 and port P4 acts as the output port. The

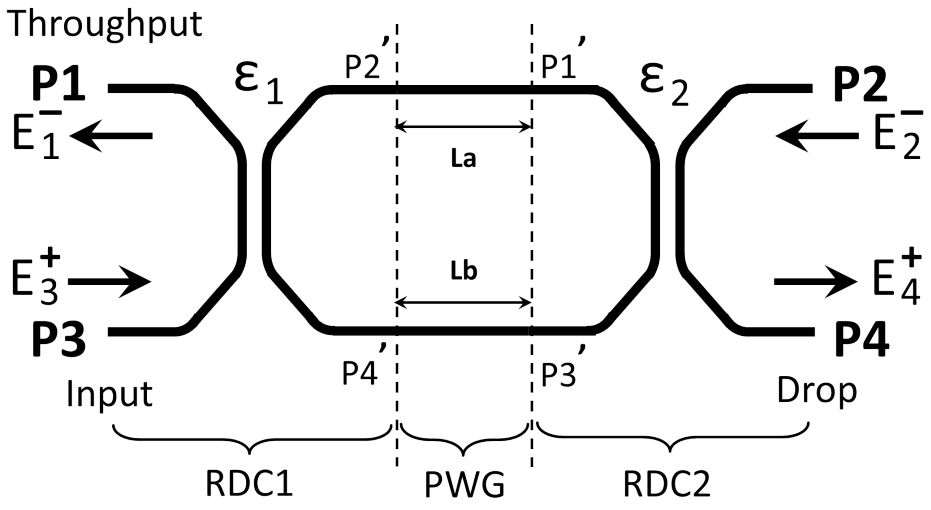

Figure 6.3: Dual-Waveguide Ring Resonator as Concatenated Structur

coupling coefficient of RDC1 is ϵ_1 and of RDC2 is ϵ_2. The waveguide in PWG is of length LA and LB along with attenuation constant α and propagation constant β.

6.2 Transfer Matrix

As previously stated in 3.1.2, the transfer matrix of the photonic device can be defined by correlating the coefficients of states on the left side of the coupling region to the coefficients of states on the right side of the coupling region. So the transfer matrix T_{RT} of a dual-waveguide ring resonator with unidirectional waveguide device in Fig. 6.3 is given as

$$\begin{bmatrix} E_4^+ \\ E_2^- \end{bmatrix} = T_{RT} \begin{bmatrix} E_3^+ \\ E_1^- \end{bmatrix}, \tag{6.1}$$

$$\begin{bmatrix} E_4^+ \\ E_2^- \end{bmatrix} = \begin{bmatrix} A & B \\ C & D \end{bmatrix} \begin{bmatrix} E_3^+ \\ E_1^- \end{bmatrix}. \tag{6.2}$$

Dual-waveguide ring resonator is comprised of 2 the rotated directional coupler with unidirectional waveguides(RDC1 and RDC2) and parallel unidirectional waveguides(PWG).

So the transfer matrix of a dual-waveguide ring resonator is combination of transfer matrices of RDC1, PWG and RDC2. So to obtain the transfer matrix of a dual-waveguide ring resonator, multiply the transfer matrices of its subsystems from right to left. So the transfer matrix T_{RT} is given as follows:

$$T_{RT} = T_{RDC2} T_{PWG} T_{RDC1}, \tag{6.3}$$

$$T_{RT} = \begin{bmatrix} A & B \\ C & D \end{bmatrix}. \tag{6.4}$$

As derived in 4.2.3, from (4.31), the transfer matrix of RDC1 and RDC2 with coupling coefficients ϵ_1 and ϵ_2 respectively is given as

$$T_{RDC1} = \frac{1}{j\sqrt{\epsilon_1}} \begin{bmatrix} -1 & \sqrt{1-\epsilon_1} \\ -\sqrt{1-\epsilon_1} & 1 \end{bmatrix}, \tag{6.5}$$

$$T_{RDC2} = \frac{1}{j\sqrt{\epsilon_2}} \begin{bmatrix} -1 & \sqrt{1-\epsilon_2} \\ -\sqrt{1-\epsilon_2} & 1 \end{bmatrix}. \tag{6.6}$$

Also as derived in 5.2.3, from (5.36), the transfer matrix of PWG is given as

$$T_{PWG} = \begin{bmatrix} e^{(-\frac{\alpha}{2}+i\beta)La} & 0 \\ 0 & e^{(\frac{\alpha}{2}-i\beta)Lb} \end{bmatrix}. \tag{6.7}$$

Substituting and multiplying T_{RDC1}, T_{RDC2} and T_{PWG} in (6.3), T_{RT} is calculated. Comparing the result with (6.4), the transmission coefficients of a dual-waveguide ring resonator the transfer matrix T_{RT} is given as follows:

$$A = \frac{-e^{-(\frac{\alpha}{2}-i\beta)La} + e^{(\frac{\alpha}{2}-i\beta)Lb}\sqrt{(1-\epsilon_1)(1-\epsilon_2)}}{\sqrt{\epsilon_1\epsilon_2}}, \tag{6.8}$$

$$B = \frac{e^{-(\frac{\alpha}{2}-i\beta)La}\sqrt{(1-\epsilon_1)} - e^{(\frac{\alpha}{2}-i\beta)Lb}\sqrt{(1-\epsilon_2)}}{\sqrt{\epsilon_1\epsilon_2}}, \tag{6.9}$$

$$C = \frac{-e^{-(\frac{\alpha}{2}-i\beta)La}\sqrt{(1-\epsilon_2)} + e^{(\frac{\alpha}{2}-i\beta)Lb}\sqrt{(1-\epsilon_1)}}{\sqrt{\epsilon_1\epsilon_2}}, \tag{6.10}$$

$$D = \frac{e^{-(\frac{\alpha}{2}-i\beta)La}\sqrt{(1-\epsilon_1)(1-\epsilon_2)} - e^{(\frac{\alpha}{2}-i\beta)Lb}}{\sqrt{\epsilon_1\epsilon_2}}. \tag{6.11}$$

So the transfer matrix parameters we are getting are equivalent to the transfer matrix parameters for two-coupler ring resonator i.e. a dual-waveguide ring resonator in [2]. They are not same as the transfer matrix concept used in [2] and concept we used is not same. In [2], coefficients of states on the right side of the coupling region are multiplied by the transfer matrix of the photonic device to get the coefficients of states on the left side of the coupling region. Opposite to this, in our derivation, coefficients of states on the left side of the coupling region are multiplied by the transfer matrix of the photonic device to get the coefficients of states on the right side of the coupling region.

6.3 Electric-Field Expressions

Electric field expression defines the analytic expression for output in device with input in device.As equation (6.2) related the input and output of a dual-waveguide ring resonator with the help of the transfer matrix, expansion of (6.2), gives electric field expression of a dual-waveguide ring resonator as follows:

$$E_4^+ = AE_3^+ + BE_1^-, \tag{6.12}$$

$$E_2^- = CE_3^+ + DE_1^-. \tag{6.13}$$

where, A, B, C and D are the transmission coefficients of a dual-waveguide ring resonators.

6.4 Performance Parameters

6.4.1 Reflection Coefficient

In a dual-waveguide ring resonator shown in fig. 6.3, port P3 acts as the input port. So some of input power from port P3 is coupled to port $P2^{'}$ and some of input power is reflected to port P1. Also some power is dissipated as a feedback from port $P4^{'}$ to port P1 in RDC1 the coupling region. So reflection of the light from the input port P3 to the throughput port P1 is given by the reflection coefficient r as follows:

$$r = \frac{E_1^-}{E_3^+}. \tag{6.14}$$

To calculate the reflection coefficient r, consider input from port P2 i.e. E_2^- is 0. So substituting this in (6.13),

$$\begin{aligned} 0 &= CE_3^+ + DE_1^-, \\ -DE_1^- &= CE_3^+, \\ \frac{E_1^-}{E_3^+} &= -\frac{C}{D}. \end{aligned} \tag{6.15}$$

So the reflection coefficient r is given as

$$r = -\frac{C}{D} \tag{6.16}$$

$$r = -\left[\frac{-e^{-(\frac{\alpha}{2}-i\beta)La}\sqrt{(1-\epsilon_2)} + e^{(\frac{\alpha}{2}-i\beta)Lb}\sqrt{(1-\epsilon_1)}}{e^{-(\frac{\alpha}{2}-i\beta)La}\sqrt{(1-\epsilon_1)(1-\epsilon_2)} - e^{(\frac{\alpha}{2}-i\beta)Lb}}\right], \tag{6.17}$$

$$r = -\left[\frac{e^{(\frac{\alpha}{2}-i\beta)Lb}\sqrt{(1-\epsilon_1)} - e^{-(\frac{\alpha}{2}-i\beta)La}\sqrt{(1-\epsilon_2)}}{-e^{(\frac{\alpha}{2}-i\beta)Lb} + e^{-(\frac{\alpha}{2}-i\beta)La}\sqrt{(1-\epsilon_1)(1-\epsilon_2)}}\right]. \tag{6.18}$$

Substitute $La = Lb = \frac{L}{2}$ and $-1 = e^{i\pi}$,

$$r = e^{i\pi}\left[\frac{e^{(\frac{\alpha L}{4})}e^{(\frac{-i\beta L}{2})}\sqrt{1-\epsilon_1} - e^{(-\frac{\alpha L}{4})}e^{(\frac{i\beta L}{2})}\sqrt{1-\epsilon_2}}{-e^{(\frac{\alpha L}{4})}e^{(\frac{-i\beta L}{2})} + e^{(-\frac{\alpha L}{4})}e^{(\frac{i\beta L}{2})}\sqrt{1-\epsilon_1}\sqrt{1-\epsilon_2}}\right], \tag{6.19}$$

$$r = e^{i(\pi+\beta L)}\left[\frac{e^{(-\frac{\alpha L}{2})}\sqrt{1-\epsilon_2} - e^{-i\beta L}\sqrt{1-\epsilon_1}}{1 - e^{(-\frac{\alpha L}{2})}e^{i\beta L}\sqrt{1-\epsilon_1}\sqrt{1-\epsilon_2}}\right]. \tag{6.20}$$

Substitute $e^{-\alpha L} = a$ and $\beta L = \phi$ and we get the reflection coefficient r for a dual-waveguide ring resonator,

$$r = e^{i(\pi+\phi)}\left[\frac{\sqrt{a}\sqrt{1-\epsilon_2} - e^{-i\phi}\sqrt{1-\epsilon_1}}{1 - \sqrt{a}e^{i\phi}\sqrt{1-\epsilon_1}\sqrt{1-\epsilon_2}}\right]. \tag{6.21}$$

Reflectivity Reflectivity R of a dual-waveguide ring resonator is given as

$$R = |r|^2, \tag{6.22}$$

$$R = r \times r^*. \tag{6.23}$$

Substitute r from (6.21) in the above equation,

$$R = \left[e^{i(\pi+\phi)}\left[\frac{\sqrt{a}\sqrt{1-\epsilon_2} - e^{-i\phi}\sqrt{1-\epsilon_1}}{1 - \sqrt{a}e^{i\phi}\sqrt{1-\epsilon_1}\sqrt{1-\epsilon_2}}\right]\right] \times \left[e^{i(\pi+\phi)}\left[\frac{\sqrt{a}\sqrt{1-\epsilon_2} - e^{-i\phi}\sqrt{1-\epsilon_1}}{1 - \sqrt{a}e^{i\phi}\sqrt{1-\epsilon_1}\sqrt{1-\epsilon_2}}\right]\right]^*,$$

$$R = \frac{a(1-\epsilon_2) - \sqrt{a(1-\epsilon_1)(1-\epsilon_2)}(e^{i\phi} + e^{-i\phi}) + (1-\epsilon_1)}{1 - \sqrt{a(1-\epsilon_1)(1-\epsilon_2)}(e^{i\phi} + e^{-i\phi}) + a(1-\epsilon_1)(1-\epsilon_2)}. \tag{6.24}$$

By Euler's formula,

$e^{i\phi} + e^{-i\phi} = 2cos(\phi)$.

Substituting this the value in the above equation, we get reflectivity R for a dual-waveguide ring resonator.

$$R = \frac{a(1-\epsilon_2) - 2\sqrt{a(1-\epsilon_1)(1-\epsilon_2)}cos(\phi) + (1-\epsilon_1)}{1 - 2\sqrt{a(1-\epsilon_1)(1-\epsilon_2)}cos(\phi) + a(1-\epsilon_1)(1-\epsilon_2)}. \tag{6.25}$$

As phase transfer functions ϕ_r is the phase difference between the input at port P3 to the output at port P1 , it is calculated from the transmission coefficient r as follows:

$$\begin{aligned}\phi_r &= arg(r),\\ \phi_r &= arg(e^{i(\pi+\phi)}\left[\frac{\sqrt{a}\sqrt{1-\epsilon_2}-e^{-i\phi}\sqrt{1-\epsilon_1}}{1-\sqrt{a}e^{i\phi}\sqrt{1-\epsilon_1}\sqrt{1-\epsilon_2}}\right]).\end{aligned} \tag{6.26}$$

6.4.2 Transmission Coefficient

In a dual-waveguide ring resonator shown in fig. 6.3, port P3 acts as the input port. Some of input power from port P3 is reflected to port P1 and some of input power is coupled to port $P2^{'}$. From port $P2^{'}$, it is induced into RDC2 through port $P1^{'}$. When the light stream is induced in the RDC2, some of power is dropped into port P4. So transmission of the light from the input port P3 to the drop port P4 is given by the transmission coefficient t as follows:

$$t = \frac{E_4^+}{E_3^+}. \tag{6.27}$$

To calculate the transmission coefficient t, substituting the value of E_1^- from (6.15) in (6.12), we get

$$\begin{aligned}E_4^+ &= AE_3^+ - \frac{BC}{D}E_3^+,\\ E_4^+ &= \frac{AD-BC}{D}E_3^+,\\ \frac{E_4^+}{E_3^+} &= \frac{AD-BC}{D},\\ t &= \frac{AD-BC}{D},\\ t &= \frac{NUM}{D}.\end{aligned} \tag{6.28}$$

where NUM = AD-BC

Substituting the value of A, B, C and D from (6.8), (6.9), (6.10) and (6.11), we get

$$NUM = \frac{[-e^{-(\frac{\alpha}{2}-i\beta)La} + e^{(\frac{\alpha}{2}-i\beta)Lb}\sqrt{(1-\epsilon_1)(1-\epsilon_2)}]}{\sqrt{\epsilon_1\epsilon_2}} \frac{[e^{-(\frac{\alpha}{2}-i\beta)La}\sqrt{(1-\epsilon_1)(1-\epsilon_2)} - e^{(\frac{\alpha}{2}-i\beta)Lb}]}{\sqrt{\epsilon_1\epsilon_2}}$$
$$- \frac{[e^{-(\frac{\alpha}{2}-i\beta)La}\sqrt{(1-\epsilon_1)} - e^{(\frac{\alpha}{2}-i\beta)Lb}\sqrt{(1-\epsilon_2)}]}{\sqrt{\epsilon_1\epsilon_2}} \frac{[-e^{-(\frac{\alpha}{2}-i\beta)La}\sqrt{(1-\epsilon_2)} + e^{(\frac{\alpha}{2}-i\beta)Lb}\sqrt{(1-\epsilon_1)}]}{\sqrt{\epsilon_1\epsilon_2}}. \tag{6.29}$$

Substitute $La = Lb = \frac{L}{2}$ and $\beta L = \phi$,

$$\begin{aligned}
NUM\epsilon_1\epsilon_2 = {} & [-e^{-(\frac{\alpha}{2}-i\beta)\frac{L}{2}} + e^{(\frac{\alpha}{2}-i\beta)\frac{L}{2}}\sqrt{(1-\epsilon_1)(1-\epsilon_2)}] \\
& [e^{-(\frac{\alpha}{2}-i\beta)\frac{L}{2}}\sqrt{(1-\epsilon_1)(1-\epsilon_2)} - e^{(\frac{\alpha}{2}-i\beta)\frac{L}{2}}] \\
& -[e^{-(\frac{\alpha}{2}-i\beta)\frac{L}{2}}\sqrt{(1-\epsilon_1)} - e^{(\frac{\alpha}{2}-i\beta)\frac{L}{2}}\sqrt{(1-\epsilon_2)}] \\
& [-e^{-(\frac{\alpha}{2}-i\beta)\frac{L}{2}}\sqrt{(1-\epsilon_2)} + e^{(\frac{\alpha}{2}-i\beta)\frac{L}{2}}\sqrt{(1-\epsilon_1)}], \\
NUM\epsilon_1\epsilon_2 = {} & [-e^{-(\frac{\alpha L}{4})}e^{(\frac{i\phi}{2})} + e^{(\frac{\alpha L}{4})}e^{-(\frac{i\phi}{2})}\sqrt{(1-\epsilon_1)(1-\epsilon_2)}] \\
& [e^{-(\frac{\alpha L}{4})}e^{(\frac{i\phi}{2})}\sqrt{(1-\epsilon_1)(1-\epsilon_2)} - e^{(\frac{\alpha L}{4})}e^{-(\frac{i\phi}{2})}] \\
& -[e^{-(\frac{\alpha L}{4})}e^{(\frac{i\phi}{2})}\sqrt{(1-\epsilon_1)} - e^{(\frac{\alpha L}{4})}e^{-(\frac{i\phi}{2})}\sqrt{(1-\epsilon_2)}] \\
& [-e^{-(\frac{\alpha L}{4})}e^{(\frac{i\phi}{2})}\sqrt{(1-\epsilon_2)} + e^{(\frac{\alpha L}{4})}e^{-(\frac{i\phi}{2})}\sqrt{(1-\epsilon_1)}].
\end{aligned} \tag{6.30}$$

Substitute $e^{-\alpha L} = a$,

$$\begin{aligned}
NUM\epsilon_1\epsilon_2 = {} & [-a^{\frac{1}{4}}e^{-\frac{i\phi}{2}} + a^{-\frac{1}{4}}e^{\frac{i\phi}{2}}\sqrt{(1-\epsilon_1)(1-\epsilon_2)}] \\
& [a^{\frac{1}{4}}e^{-\frac{i\phi}{2}}\sqrt{(1-\epsilon_1)(1-\epsilon_2)} - a^{-\frac{1}{4}}e^{\frac{i\phi}{2}}] \\
& -[a^{\frac{1}{4}}e^{-\frac{i\phi}{2}}\sqrt{(1-\epsilon_1)} - a^{-\frac{1}{4}}e^{\frac{i\phi}{2}}\sqrt{(1-\epsilon_2)}] \\
& [-a^{\frac{1}{4}}e^{-\frac{i\phi}{2}}\sqrt{(1-\epsilon_2)} + a^{-\frac{1}{4}}e^{\frac{i\phi}{2}}\sqrt{(1-\epsilon_1)}], \\
NUM = {} & 1.
\end{aligned} \tag{6.31}$$

Substituting $NUM = 1$ and the value of D from (6.11) in (6.28), the transmission coefficient t is given as

$$t = \frac{\sqrt{\epsilon_1\epsilon_2}}{e^{-(\frac{\alpha}{2}-i\beta)La}\sqrt{(1-\epsilon_1)(1-\epsilon_2)} - e^{(\frac{\alpha}{2}-i\beta)Lb}}. \tag{6.32}$$

Substitute $La = Lb = \frac{L}{2}$,

$$t = \frac{\sqrt{\epsilon_1\epsilon_2}}{e^{-(\frac{\alpha}{2}-i\beta)\frac{L}{2}}\sqrt{(1-\epsilon_1)(1-\epsilon_2)} - e^{(\frac{\alpha}{2}-i\beta)\frac{L}{2}}},$$
$$t = e^{i(\pi+\beta L)}\frac{\sqrt{\epsilon_1\epsilon_2}e^{-\frac{\alpha L}{4}}e^{-\frac{i\beta L}{2}}}{1 - e^{-\frac{\alpha L}{2}}e^{i\beta L}\sqrt{(1-\epsilon_1)(1-\epsilon_2)}}. \tag{6.33}$$

Substituting $a = e^{-\alpha L}$ and $\phi = \beta L$, we get the transmission coefficient t of a dual-waveguide ring resonator as follows:

$$t = e^{i(\pi+\phi)}\frac{\sqrt[4]{a}\sqrt{\epsilon_1\epsilon_2}e^{-\frac{i\phi}{2}}}{1 - \sqrt{a}e^{i\phi}\sqrt{(1-\epsilon_1)(1-\epsilon_2)}}. \tag{6.34}$$

Transmittivity T of a dual-waveguide ring resonator is given as

$$T = |t|^2, \tag{6.35}$$
$$T = t \times t^*. \tag{6.36}$$

Substitute t from (6.34) in the above equation, we get transmittivity T of a dual-waveguide ring resonator

$$T = \left[e^{i(\pi+\phi)} \frac{\sqrt[4]{a}\sqrt{\epsilon_1\epsilon_2}e^{-\frac{i\phi}{2}}}{1-\sqrt{a}e^{i\phi}\sqrt{(1-\epsilon_1)(1-\epsilon_2)}} \right] \times \left[e^{i(\pi+\phi)} \frac{\sqrt[4]{a}\sqrt{\epsilon_1\epsilon_2}e^{-\frac{i\phi}{2}}}{1-\sqrt{a}e^{i\phi}\sqrt{(1-\epsilon_1)(1-\epsilon_2)}} \right]^*,$$

$$T = \left[e^{i(\pi+\phi)} \frac{\sqrt[4]{a}\sqrt{\epsilon_1\epsilon_2}e^{-\frac{i\phi}{2}}}{1-\sqrt{a}e^{i\phi}\sqrt{(1-\epsilon_1)(1-\epsilon_2)}} \right] \times \left[e^{-i(\pi+\phi)} \frac{\sqrt[4]{a}\sqrt{\epsilon_1\epsilon_2}e^{\frac{i\phi}{2}}}{1-\sqrt{a}e^{-i\phi}\sqrt{(1-\epsilon_1)(1-\epsilon_2)}} \right],$$

$$T = \frac{\sqrt{a}\epsilon_1\epsilon_2}{1-2\sqrt{a(1-\epsilon_1)(1-\epsilon_2)}cos(\phi)+a(1-\epsilon_1)(1-\epsilon_2)},$$

$$T = \frac{\sqrt{a}\epsilon_1\epsilon_2}{1-2\sqrt{a(1-\epsilon_1)(1-\epsilon_2)}+2\sqrt{a(1-\epsilon_1)(1-\epsilon_2)}-2\sqrt{a(1-\epsilon_1)(1-\epsilon_2)}cos(\phi)+a(1-\epsilon_1)(1-\epsilon_2)},$$

$$T = \frac{\sqrt{a}\epsilon_1\epsilon_2}{1-2\sqrt{a(1-\epsilon_1)(1-\epsilon_2)}+a(1-\epsilon_1)(1-\epsilon_2)+2\sqrt{a(1-\epsilon_1)(1-\epsilon_2)}(1-cos(\phi))},$$

$$T = \frac{\sqrt{a}\epsilon_1\epsilon_2}{(1-\sqrt{a(1-\epsilon_1)(1-\epsilon_2)})^2+4\sqrt{a(1-\epsilon_1)(1-\epsilon_2)}sin^2(\frac{\phi}{2}))}. \quad (6.37)$$

So the transmittivity we are getting is same as transmittivity for two-coupler ring resonator i.e. a dual-waveguide ring resonator in [2], even the transfer matrix concept used in [2] and concept we used is not same. Because the transmittivity is the fraction of power transmitted from the input port to the output port passing through the coupling region of coupler and power transfer will be same in both cases.

As phase transfer functions ϕ_t is the phase difference between the input at port P3 to the output at port P4 , it is calculated from the transmission coefficient r as follows:

$$\phi_t = arg(t),$$
$$\phi_t = arg(e^{i(\pi+\phi)} \frac{\sqrt[4]{a}\sqrt{\epsilon_1\epsilon_2}e^{-\frac{i\phi}{2}}}{1-\sqrt{a}e^{i\phi}\sqrt{(1-\epsilon_1)(1-\epsilon_2)}}). \quad (6.38)$$

6.5 Performance Parameters Spectra

6.5.1 Reflectivity and Transmittivity Spectra

As seen in (6.25) and (6.37), reflectivity and transmittivity of a dual-waveguide ring resonator is dependent upon various parameters such as ϵ_1, ϵ_2, α, β and L. The following various graphs shows how reflectivity and transmittivity varies with different parameters.

Reflectivity and Transmittivity vs. ϵ_1

The graph in Fig. 6.4 shows how reflectivity R and transmittivity T varies with ϵ_1. For this graph, only ϵ_1 is varied and other values used are $\epsilon_2 = 0.5$, $\beta L = \frac{\pi}{2}$, $a = 0.95$.

As seen in Fig. 6.4, R decreases as ϵ increases whereas T increases with ϵ.

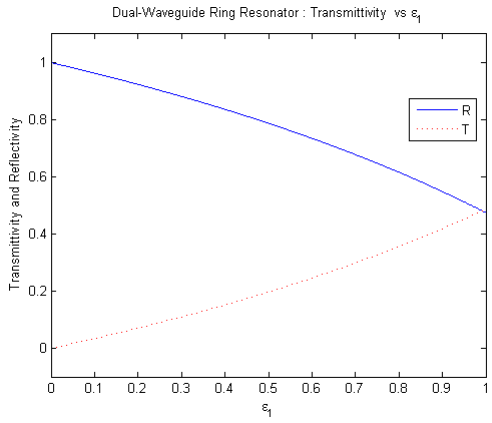

Figure 6.4: Reflectivity and Transmittivity vs. ϵ_1

Reflectivity and Transmittivity vs. ϵ_2

The graph in Fig. 6.5 shows how reflectivity R and transmittivity T varies with ϵ_2. For this graph, only ϵ_2 is varied and others the value used are as follows:
$\epsilon_1 = 0.5$, $\beta L = \frac{\pi}{2}$, $a = 0.95$.

As seen in Fig. 6.5, R decreases as ϵ increases whereas T increases with ϵ.

Reflectivity vs. $\frac{\beta L}{\pi}$ **- For various values of** ϵ_1

The graph in Fig. 6.6 shows how reflectivity R varies with normalized frequency $\frac{\beta L}{\pi}$. For this graph, only $\frac{\beta L}{\pi}$ is varied for different values of ϵ_1 and other values used are $\epsilon_2 = 0.5$, $a = 0.95$.

As seen in Fig. 6.6, reflectivity R remains constant 1 when the coupling coefficient for RDC1 ϵ_1 is 0 as all power is transferred from port P3 to port P1. Graph also shows how reflectivity R varies for $\epsilon_1 = 0.5$ and $\epsilon_1 = 0.9$.

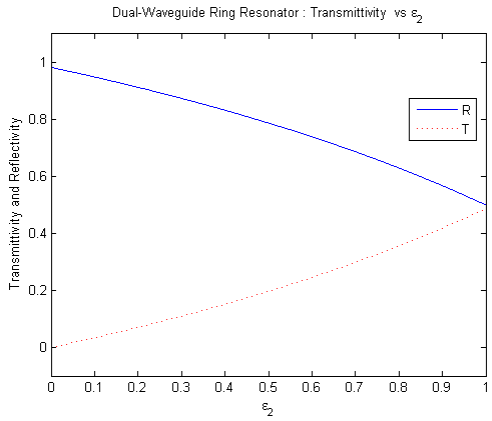

Figure 6.5: Reflectivity and Transmittivity vs. ϵ_2

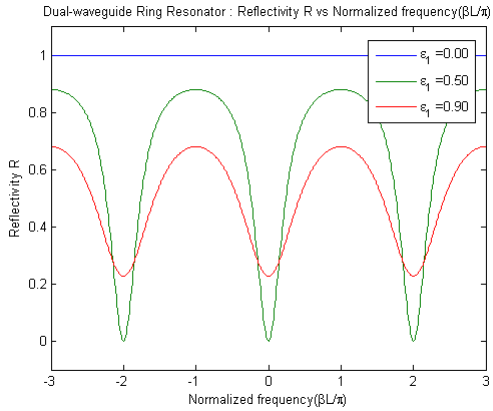

Figure 6.6: Reflectivity vs. $\frac{\beta L}{\pi}$

Transmittivity vs. $\frac{\beta L}{\pi}$ - For various values of ϵ_1

The graph in Fig. 6.7 shows how transmittivity T varies with normalized frequency $\frac{\beta L}{\pi}$. For this graph, only $\frac{\beta L}{\pi}$ is varied for different values of ϵ_1 and other values used are $\epsilon_2 = 0.5$, $a = 0.95$.

As seen in Fig. 6.7, transmittivity T is 0 when the coupling coefficient for RDC1 ϵ_1 is 0 as all power is transferred from port P3 to port P1, there is no power dissipated at port P4 . Graph also shows how reflectivity R varies for $\epsilon_1 = 0.5$ and $\epsilon_1 = 0.9$.

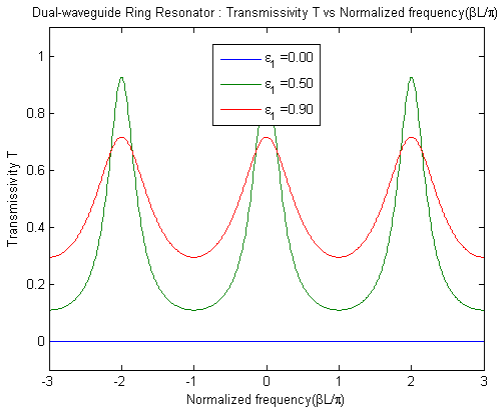

Figure 6.7: Transmittivity vs. $\frac{\beta L}{\pi}$

Reflectivity vs. $\frac{\beta L}{\pi}$ - For various values of ϵ_2

The graph in Fig. 6.8 shows how reflectivity R varies with normalized frequency $\frac{\beta L}{\pi}$. For this graph, only $\frac{\beta L}{\pi}$ is varied for different values of ϵ_2 and other values used are $\epsilon_1 = 0.5$, $a = 0.95$.

As seen in Fig. 6.8, as ϵ_2 increases from 0 to 0.5, trough increases but troughs start decreasing again as ϵ_2 increases from 0.5 onward.

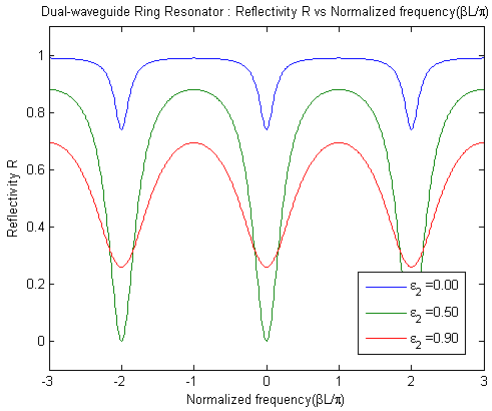

Figure 6.8: Reflectivity vs. $\frac{\beta L}{\pi}$

Transmittivity vs. $\frac{\beta L}{\pi}$ - For various values of ϵ_2

The graph in Fig. 6.9 shows how transmittivity T varies with normalized frequency $\frac{\beta L}{\pi}$. For this graph, only $\frac{\beta L}{\pi}$ is varied for different values of ϵ_2 and other values used are $\epsilon_1 = 0.5$, $a = 0.95$.

As seen in Fig. 6.9, as ϵ_2 increases from 0 to 0.5, peak starts increasing but peak start decreasing again as ϵ_2 increases from 0.5 onward.

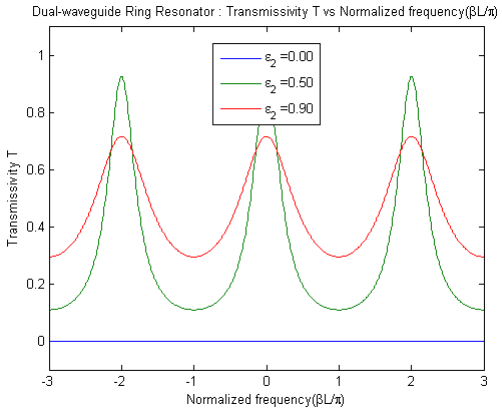

Figure 6.9: Transmittivity vs. $\frac{\beta L}{\pi}$

6.5.2 Phase Transfer Function Spectra

As seen in (6.27) and (6.38), the phase transfer function of a dual-waveguide ring resonator is dependent upon various parameters such as ϵ_1, ϵ_2, α, β and L. The following various graphs shows how phase transfer functions varies with different parameters.

Phase Transfer Function vs. ϵ_1

The graph in Fig. 6.10 shows how phase transfer functions varies with ϵ_1. For this graph, only ϵ_1 is varied and other values used are $\epsilon_2 = 0.5$, $\beta L = \frac{\pi}{2}$, $a = 0.95$

As seen in Fig. 6.10, phase ϕ_r changes from 0 to $-\frac{\pi}{2}$ as ϵ_1 increases similarly ϕ_t changes as ϵ_1 increases .

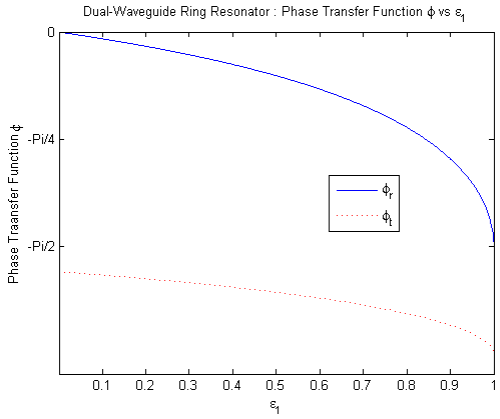

Figure 6.10: Phase Transfer Function vs. ϵ_1

Phase Transfer Function vs. ϵ_2

The graph in Fig. 6.11 shows how phase transfer functions varies with ϵ_2. For this graph, only ϵ_2 is varied and other values used are $\epsilon_1 = 0.5$, $\beta L = \frac{\pi}{2}$, $a = 0.95$.

As seen in Fig. 6.11, phase ϕ_r moves towards 0 as ϵ_2 increases whereas ϕ_t moves in opposite direction as ϵ_2 increases .

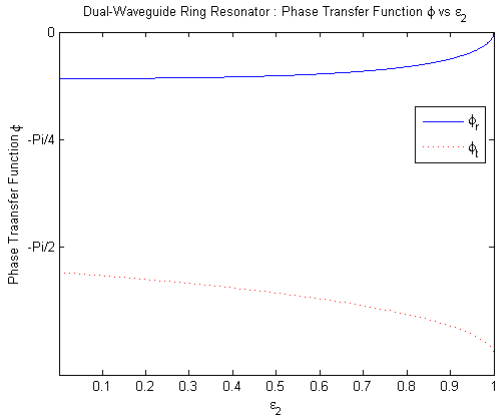

Figure 6.11: Phase Transfer Function vs. ϵ_2

Phase Transfer Function ϕ_r **vs.** $\frac{\beta L}{\pi}$ **- For various values of** ϵ_1

The graph in Fig. 6.12 shows how the phase transfer function ϕ_r varies with normalized frequency $\frac{\beta L}{\pi}$. For this graph, only $\frac{\beta L}{\pi}$ is varied for different values of ϵ_1 and other values

used are $\epsilon_2 = 0.5$, $a = 0.95$.

As seen in Fig. 6.12, the phase transfer function ϕ_r remains constant 1 when the coupling coefficient for RDC1 ϵ_1 is 0 as all power is transferred from port P3 to port P1. Graph also shows how reflectivity R varies for $\epsilon_1 = 0.5$ and $\epsilon_1 = 0.9$.

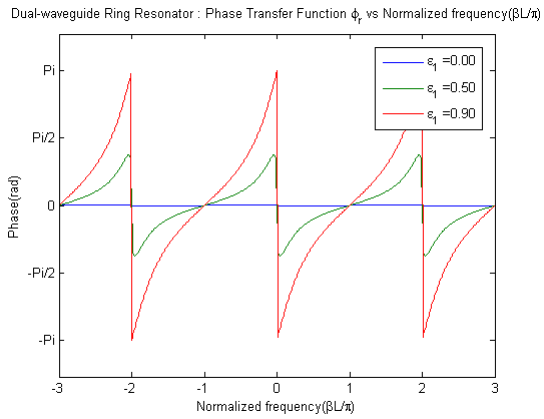

Figure 6.12: Phase Transfer Function ϕ_r vs. $\frac{\beta L}{\pi}$

Phase Transfer Function ϕ_t vs. $\frac{\beta L}{\pi}$ - For various values of ϵ_1

The graph in Fig. 6.13 shows how the phase transfer function ϕ_t varies with normalized frequency $\frac{\beta L}{\pi}$. For this graph, only $\frac{\beta L}{\pi}$ is varied for different values of ϵ_1 and other values used are $\epsilon_2 = 0.5$, $a = 0.95$.

Graph shows how the phase transfer function ϕ_t varies for various values $\epsilon_1 = 0$, $\epsilon_1 = 0.5$ and $\epsilon_1 = 0.9$.

Phase Transfer Function ϕ_r vs. $\frac{\beta L}{\pi}$ - For various values of ϵ_2

The graph in Fig. 6.14 shows how the phase transfer function ϕ_r varies with normalized frequency $\frac{\beta L}{\pi}$. For this graph, only $\frac{\beta L}{\pi}$ is varied for different values of ϵ_2 and other values used are $\epsilon_1 = 0.5$, $a = 0.95$.

Graph shows how the phase transfer function ϕ_r varies for various values $\epsilon_2 = 0$, $\epsilon_2 = 0.5$ and $\epsilon_2 = 0.9$.

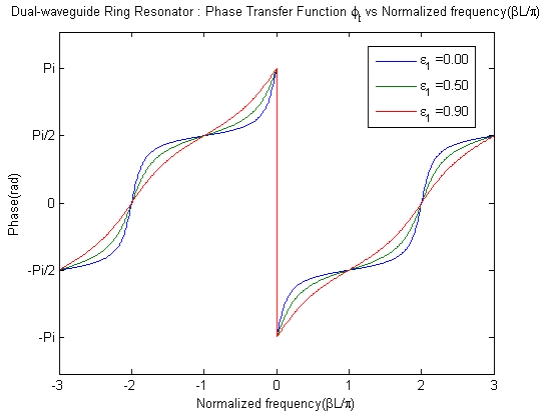

Figure 6.13: Phase Transfer Function ϕ_t vs. $\frac{\beta L}{\pi}$

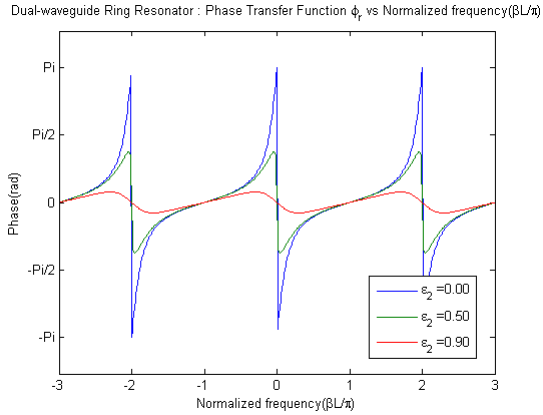

Figure 6.14: Phase Transfer Function ϕ_r vs. $\frac{\beta L}{\pi}$

Phase Transfer Function ϕ_t vs. $\frac{\beta L}{\pi}$ - For various values of ϵ_2

The graph in Fig. 6.14 shows how the phase transfer function ϕ_t varies with normalized frequency $\frac{\beta L}{\pi}$. For this graph, only $\frac{\beta L}{\pi}$ is varied for different values of ϵ_2 and other values used are $\epsilon_1 = 0.5$, $a = 0.95$.

Graph shows how the phase transfer function ϕ_t varies for various values $\epsilon_2 = 0$, $\epsilon_2 = 0.5$ and $\epsilon_2 = 0.9$.

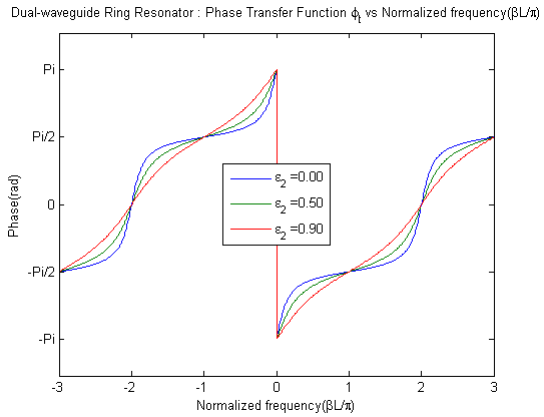

Figure 6.15: Phase Transfer Function ϕ_t vs. $\frac{\beta L}{\pi}$

Chapter 7

Ring Resonator

7.1 Introduction

7.1.1 Ring Resonator

A ring resonator is similar to a dual-waveguide ring resonator with a difference of a waveguide. A ring resonator can be designed, as shown in Fig. 7.1(a), by placing the photonic ring near a photonic waveguide creating a coupling region between a ring and waveguide. We can also say that "a ring resonator can be designed by connecting the input and output ports associated with one core of a directional coupler through a piece of fiber to form a ring" [1]. The significant property of this device is that the light propagates only in one direction i.e. the forward direction. For lossless conditions, all input power is transmitted to the output. So this device is also called as the *all-pass* filter.

As seen in Fig. 7.1(a), there are two ports in the device. When the light is entered in the input port as seen in Fig. 7.1(a), it travels towards the coupling region with coupling coefficient ϵ_1. When it reaches the coupling region with coupling coefficient ϵ_1, some quantity of the power from the input port is coupled into the ring and the remaining power is dissipated at the throughput port. The power coupled into the ring travels in the ring till it reaches back to the coupling region. At this point it again combines with the power from the input port and some of the power is coupled to the throughput region whereas some of it is re-transmitted into the ring. So some quantity of power keeps circulating in the ring which generates resonances.

From Fig. 7.1(a), it can be observed that the ring resonator has a coupling region with

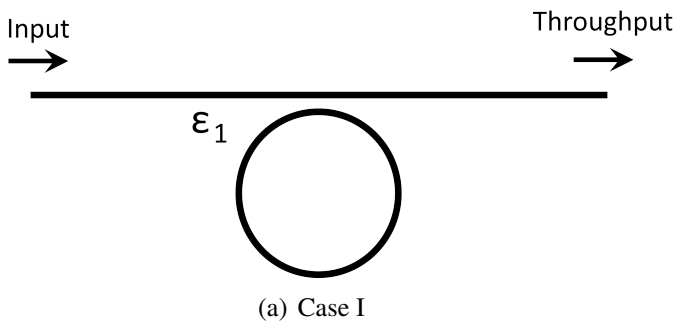

(a) Case I

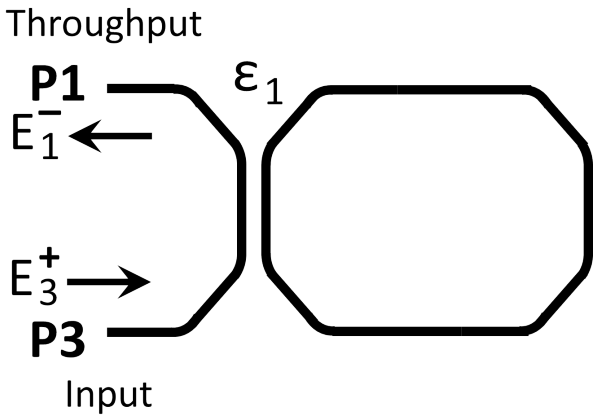

(b) Case II

Figure 7.1: Ring Resonator

coupling coefficient ϵ_1. As stated above, this coupling region forms a directional coupler. Rotating Fig. 7.1(a) 90^o counter-clockwise and arranging a coupling region as a rotated directional coupler, we get Fig. 7.1(b). So Fig. 7.1(b) is the ring resonator which is arranged in the different style.

7.1.2 Ring Resonator with Ghost Waveguide

As described in chapter 4, a *ghost* waveguide is a waveguide which is fabricated for the purpose of convenience. So let's introduce a ghost waveguide in Fig. 7.1(b) which forms a coupling region with the ring but in the opposite side of the present coupling region. This use of the ghost waveguide transform the ring resonator in Fig. 7.1(a) into Fig. 7.2. But Fig. 7.2 is the same as a dual-waveguide ring resonator in Fig. 6.3. From Fig. 7.2, it can be

observed that, a ring resonator (with the ghost waveguide) is obtained by a concatenation of a rotated directional coupler, parallel waveguides and another rotated directional coupler. As there are two rotated directional couplers, define a rotated directional coupler on the left as *RDC1* and rotated directional coupler on the right as *RDC2*.Lets define the parallel waveguides as *PWG*.

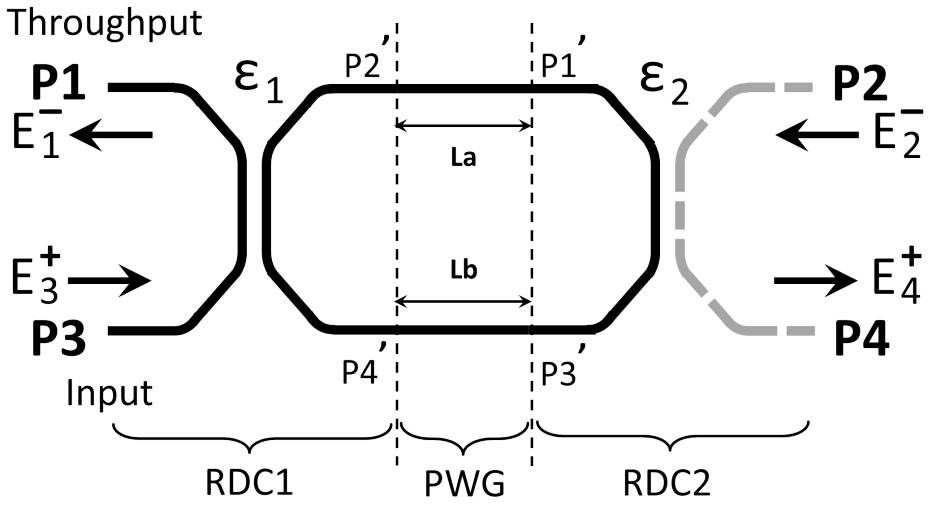

Figure 7.2: Ring Resonator with Ghost Waveguide

As seen in Fig. 7.2, RDC1 has four ports P1, P3, $P2^{'}$ and $P4^{'}$. Similarly, ports for RDC2 are designated as P2, P4, $P1^{'}$ and $P4^{'}$. But for the overall coupled structure i.e. ring resonator (with ghost waveguide), the four ports are P1, P2, P3 and P4. Field at P1, P2, P3 and P4 is given by E_1^-, E_2^-, E_3^+ and E_4^+ respectively. For the ring resonator (with the ghost waveguide), port P3 and P2 acts as the input port and port P1 and port P4 acts as the output port. The coupling coefficient of RDC1 is ϵ_1 and of RDC2 is ϵ_2. The waveguide in PWG is of length La and Lb along with the attenuation constant α and propagation constant β. As the RDC2 is formed with the help of a ghost waveguide for mathematical convenience, the coupling coefficient of RDC2 is ϵ_2 will be taken as 0 at the appropriate section ahead.

7.2 Transfer Matrix

As previously stated in 3.1.2, the transfer matrix of the photonic device can be defined by correlating the coefficients of states on the left side of the coupling region to the coefficients of states on the right side of the coupling region. So the transfer matrix T_{RR} of the ring resonator(with the ghost waveguide) device in Fig. 7.2 is given as

$$\begin{bmatrix} E_4^+ \\ E_2^- \end{bmatrix} = T_{RR} \begin{bmatrix} E_3^+ \\ E_1^- \end{bmatrix}, \tag{7.1}$$

$$\begin{bmatrix} E_4^+ \\ E_2^- \end{bmatrix} = \begin{bmatrix} A & B \\ C & D \end{bmatrix} \begin{bmatrix} E_3^+ \\ E_1^- \end{bmatrix}. \tag{7.2}$$

The ring resonator(with the ghost waveguide) is comprised of 2 the rotated directional coupler with unidirectional waveguides(RDC1 and RDC2) and parallel unidirectional waveguides(PWG). So the transfer matrix of the ring resonator(with the ghost waveguide) is combination of transfer matrices of RDC1, PWG and RDC2. So to obtain the transfer matrix of the ring resonator(with the ghost waveguide), multiply the transfer matrices of its subsystems from right to left. So the transfer matrix T_{RR} is given as follows:

$$T_{RR} = T_{RDC2} T_{PWG} T_{RDC1}, \tag{7.3}$$

$$T_{RR} = \begin{bmatrix} A & B \\ C & D \end{bmatrix}. \tag{7.4}$$

But a device in Fig. 7.2 is the same as a device in Fig. 7.1(b). As (7.3) is the same as (6.3), the transfer matrix of both devices is the same. So from (6.4), (6.8), (6.9), (6.10), and (6.11), the transfer matrix T_{RR} of the ring resonator(with the ghost waveguide) with the unidirectional waveguide device in Fig. 7.2 is given as

$$T_{RT} = \begin{bmatrix} A & B \\ C & D \end{bmatrix}. \tag{7.5}$$

where,

$$A = \frac{-e^{-(\frac{\alpha}{2}-i\beta)La} + e^{(\frac{\alpha}{2}-i\beta)Lb}\sqrt{(1-\epsilon_1)(1-\epsilon_2)}}{\sqrt{\epsilon_1\epsilon_2}}, \tag{7.6}$$

$$B = \frac{e^{-(\frac{\alpha}{2}-i\beta)La}\sqrt{(1-\epsilon_1)} - e^{(\frac{\alpha}{2}-i\beta)Lb}\sqrt{(1-\epsilon_2)}}{\sqrt{\epsilon_1\epsilon_2}}, \tag{7.7}$$

$$C = \frac{-e^{-(\frac{\alpha}{2}-i\beta)La}\sqrt{(1-\epsilon_2)} + e^{(\frac{\alpha}{2}-i\beta)Lb}\sqrt{(1-\epsilon_1)}}{\sqrt{\epsilon_1\epsilon_2}}, \tag{7.8}$$

$$D = \frac{e^{-(\frac{\alpha}{2}-i\beta)La}\sqrt{(1-\epsilon_1)(1-\epsilon_2)} - e^{(\frac{\alpha}{2}-i\beta)Lb}}{\sqrt{\epsilon_1\epsilon_2}}. \tag{7.9}$$

7.3 Electric-Field Expressions

Electric field expressions define the analytic expression for output in a device with input in a device. A device is Fig. 7.2 is the same as a device in Fig. 6.3. So electric field expressions of both devices are the same. So (6.12) and (6.13) give electric field expressions of a dual-waveguide ring resonator(with the ghost waveguide) as follows:

$$E_4^+ = AE_3^+ + BE_1^-, \tag{7.10}$$

$$E_2^- = CE_3^+ + DE_1^-. \tag{7.11}$$

where, A, B, C and D are the transmission coefficients of a dual-waveguide ring resonators.

7.4 Performance Parameters

7.4.1 Reflection Parameters

In the ring resonator (with the ghost waveguide) shown in fig. 7.2, port P3 acts as the input port. So some of input power from port P3 is coupled to port $P2^{'}$ and some of input power is reflected to port P1. Also some power is dissipated as a feedback from port $P4^{'}$ to port

P1 in the RDC1 coupling region. So reflection of the light from the input port P3 to the throughput port P1 is given by the reflection coefficient r as follows:

$$r = \frac{E_1^-}{E_3^+}. \tag{7.12}$$

The transfer matrix of the ring resonator (with the ghost waveguide) and the dual-waveguide ring resonator is the same as well as the reflection coefficient in (7.12) and (6.14) is the same. So the reflection coefficient for the ring resonator with (the ghost waveguide) is the same as the reflection coefficient for the dual-waveguide ring resonator. So from (6.21), the reflection coefficient for the ring resonator with (the ghost waveguide) can be written as,

$$r = e^{i(\pi+\phi)} \left[\frac{\sqrt{a}\sqrt{1-\epsilon_2} - e^{-i\phi}\sqrt{1-\epsilon_1}}{1 - \sqrt{a}e^{i\phi}\sqrt{1-\epsilon_1}\sqrt{1-\epsilon_2}} \right]. \tag{7.13}$$

As discussed above, the ghost waveguide is used for the sake of calculation convenience. So to eliminate RDC2 and convert the ring resonator with (the ghost waveguide) to the ring resonator, consider $\epsilon_2 = 0$. As there is no coupling at the RDC2 coupling region, all power reached at port $P1^{'}$ is dissipated at port $P3^{'}$. So substituting $\epsilon_2 = 0$ in the above equation, we get the reflection coefficient for the ring resonator as follows:

$$r = e^{i(\pi+\phi)} \left[\frac{\sqrt{a} - e^{-i\phi}\sqrt{1-\epsilon_1}}{1 - \sqrt{a}e^{i\phi}\sqrt{1-\epsilon_1}} \right]. \tag{7.14}$$

The reflection coefficient we are getting is the same as the reflection coefficient for the ring resonator in Ref. [1].

Reflectivity Similar to the reflection coefficient, the reflectivity of the ring resonator can be derived by substituting $\epsilon_2 = 0$ in (6.37). So the reflectivity of the ring resonator is given as

$$R = \frac{a - 2\sqrt{a(1-\epsilon_1)}cos(\phi) + (1-\epsilon_1)}{1 - 2\sqrt{a(1-\epsilon_1)}cos(\phi) + a(1-\epsilon_1)}. \tag{7.15}$$

The reflectivity we are getting is the same as the transmission past the resonator in the input waveguide for the ring resonator in Ref. [11].

Phase Transfer Function Similar to the reflection coefficient, the phase transfer function of the ring resonator can be derived by substituting $\epsilon_2 = 0$ in (6.38). So the phase transfer function of the ring resonator is given as

$$\begin{aligned} &\phi_r = arg(r) \\ &\phi_r = arg(e^{i(\pi+\phi)} \left[\frac{\sqrt{a} - e^{-i\phi}\sqrt{1-\epsilon_1}}{1 - \sqrt{a}e^{i\phi}\sqrt{1-\epsilon_1}}\right]). \end{aligned} \tag{7.16}$$

7.4.2 Transmission Parameters

As in the ring resonator shown in Fig. 7.1, all power from the input port is transferred to the throughput port. But the ring resonator (with the ghost waveguide) is the same as the dual-waveguide ring resonator. As we assumed $\epsilon_2 = 0$ to convert the ring resonator (with the ghost waveguide) to the ring resonator, it is necessary to verify that no power is leaked at port P4 in Fig. 7.2. So transmission of the light from the input port P3 to the drop port P4, given by the transmission coefficient t is calculated by substituting $\epsilon_2 = 0$ in (6.34). So transmission of the light from the input port P3 to the drop port P4 in the ring resonator(with the ghost waveguide) is given as

$$\begin{aligned} &t = e^{i(\pi+\phi)} \frac{\sqrt[4]{a}\sqrt{\epsilon_1 * 0}e^{-\frac{i\phi}{2}}}{1 - \sqrt{a}e^{i\phi}\sqrt{(1-\epsilon_1)(1-0)}}, \\ &t = 0. \end{aligned} \tag{7.17}$$

So, there is no transmission of the light from the input port P3 to the drop port P4 in the ring resonator(with the ghost waveguide) i.e. no there is no power loss through the ghost waveguide in the ring resonator. As the transmission coefficient is 0, the transmittivity is 0.

7.5 Performance Parameters Spectra

7.5.1 Reflectivity Spectra

As seen in (7.15), the reflectivity of the ring resonator is dependent upon various parameters such as ϵ_1, α, β and L. The following various graphs shows how the reflectivity varies with different parameters.

Reflectivity vs. ϵ_1

The graph in Fig. 7.3 shows how the reflectivity R varies with ϵ_1. For this graph, only ϵ_1 is varied and other values used are $\beta L = \frac{\pi}{2}$ and $a = 0.95$.

As seen in Fig. 7.3, R decreases as ϵ_1 increases. Also it can be observed that T remains 0 independent of value of ϵ_1.

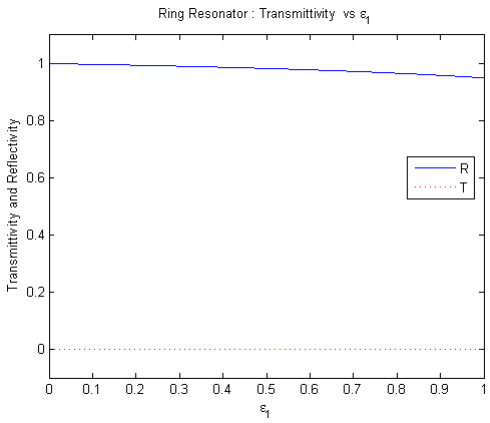

Figure 7.3: Reflectivity vs. ϵ_1

Reflectivity vs. $\frac{\beta L}{\pi}$

The graph in Fig. 7.4 shows how the reflectivity R varies with normalized frequency $\frac{\beta L}{\pi}$. For this graph, only $\frac{\beta L}{\pi}$ is varied for different values of ϵ_1 and other value used is $a = 0.95$.

As seen in Fig. 7.4, as ϵ_1 decreases, the resonances becomes sharper. Resonances gets sharper at $\epsilon_1 = 0.10$

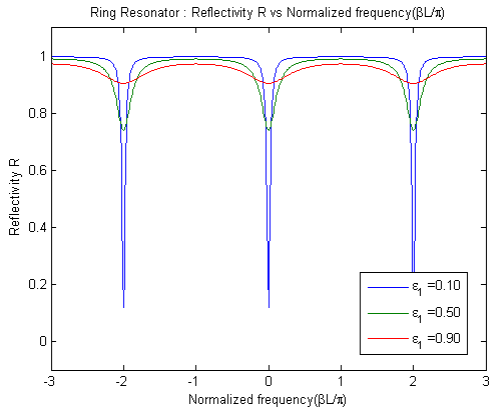

Figure 7.4: Reflectivity vs. $\frac{\beta L}{\pi}$

7.5.2 Phase Transfer Function Spectra

As seen in (7.16) , the phase transfer function of the ring resonator is dependent upon various parameters such as ϵ_1, α, β and L. The following various graphs shows how the phase transfer function varies with different parameters.

Phase Transfer Function vs. ϵ

The graph in Fig. 7.5, shows how phase transfer functions varies with ϵ_1. For this graph, only ϵ_1 is varied and other values used are $\beta L = \frac{\pi}{2}$ and $a = 0.95$.

As seen in Fig. 7.5, phase ϕ_r changes from 0 to $-\frac{\pi}{2}$ as ϵ_1 increases.

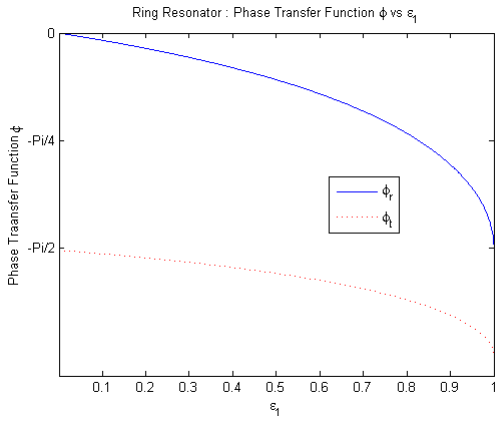

Figure 7.5: Phase Transfer Function vs. ϵ

Phase Transfer Function ϕ_r vs. $\frac{\beta L}{\pi}$

The graph in Fig. 7.6 shows how the phase transfer function ϕ_r varies with normalized frequency $\frac{\beta L}{\pi}$. For this graph, only $\frac{\beta L}{\pi}$ is varied for different values of ϵ_1 and other values used are $a = 0.95$.

As seen in Fig. 7.6, the graph also shows how the reflectivity R varies for $\epsilon_1 = 0.10$, $\epsilon_1 = 0.5$ and $\epsilon_1 = 0.9$.

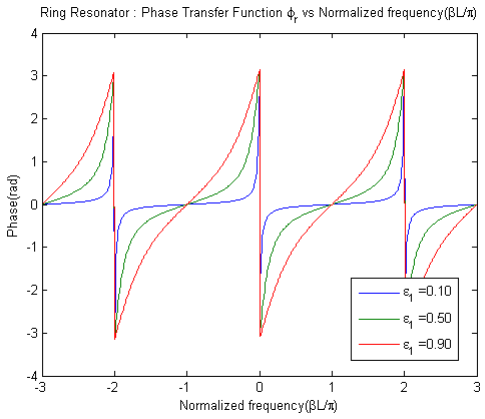

Figure 7.6: Phase Transfer Function ϕ_r vs. $\frac{\beta L}{\pi}$

7.6 Significance of Ghost Waveguide Coupling Coefficient

As seen in the section 7.5, the ghost waveguide is eliminated to remodel the Fig. 7.2 into the ring resonator and the performance parameters of the ring resonator is obtained by substituting the value of the coupling coefficient $\epsilon_2 = 0$ in the dual-waveguide ring resonator performance parameters. This coupling coefficient represents the coupling between the ring and the ghost waveguide.

7.6.1 Ghost Waveguide Coupling Coefficient $\epsilon_2 = 0$

We substituted this $\epsilon_2 = 0$ while calculating performance parameters of the device. We could have substituted $\epsilon_2 = 0$ either before transfer matrix multiplication or immediately after transfer matrix multiplication to simplify equation. If we substituted $\epsilon_2 = 0$ before

the transfer matrix multiplication, then we need to substitute it in the transfer matrix of the rotated directional coupler. But in the transfer matrix of the rotated directional coupler, there is ϵ term in the denominator which turns the transfer matrix of the rotated directional coupler to infinity. Similarly if we substituted $\epsilon_2 = 0$ in the transfer matrix of the ring resonator(with the ghost waveguide), it could have turned the transfer matrix of the rotated directional coupler to infinity. So we couldn't substitute $\epsilon_2 = 0$ either before the transfer matrix multiplication or immediately after transfer matrix multiplication. We substituted $\epsilon_2 = 0$ in transfer matrix parameter equations and we got the above performance parameters for the ring resonator.

7.6.2 Impact of Ghost Waveguide Coupling Coefficient ϵ_2 on Reflectivity

The ghost waveguide coupling coefficient ϵ_2 has a lot of impact on the reflectivity of the ring resonator. If the ghost waveguide coupling coefficient ϵ_2 varies from 0, then there is some power dissipation through the RDC2. The impact of the ghost waveguide coupling coefficient ϵ_2 on the reflectivity R and the phase transfer function ϕ_r is shown in following graphs.

The graphs in Fig. 7.7 and Fig. 7.8 shows the impact of the ghost waveguide coupling coefficient ϵ_2 on the reflectivity R. In these graphs, the reflectivity R is plotted against the normalized frequency βL and graphs are plotted for various values of ϵ_2. The value of ϵ_1 in both graphs is 0.5 but $a = 1$ i.e. lossless device for the graph in Fig 7.7 and $a = 0.95$ for the graph in Fig 7.8.

As seen in Fig 7.7, the reflectivity R is constant 1 for $\epsilon_2 = 0$ but as the value of ϵ_2 increases the resonances start evolving which goes on increasing. Similarly, in Fig/ 7.9, the resonances start evolving for $\epsilon_2 = 0$ and the resonances become sharper as $\epsilon_2 = 0$ increases to $\epsilon_2 = 0.5$. In Fig/ 7.8, the resonances starts evolving for $\epsilon_2 = 0$ due to attenuation in the parallel waveguides and as the coupling coefficient $\epsilon_2 = 0$ increases the resonances becomes sharper due to power dissipation through the ghost waveguide.

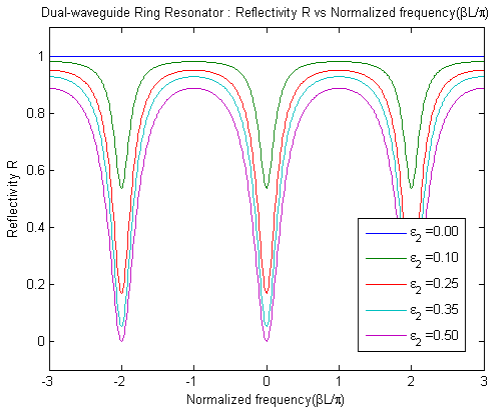

Figure 7.7: Reflectivity R vs. ϵ_1

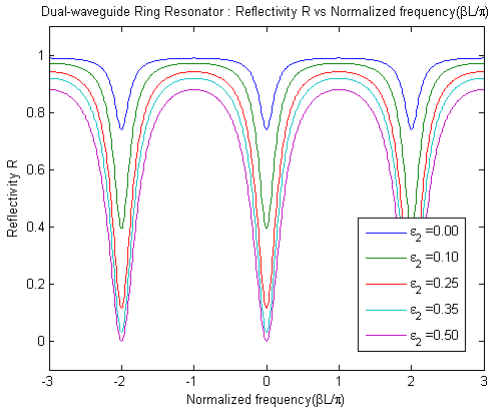

Figure 7.8: Reflectivity R vs. ϵ_1

The graphs in Fig. 7.9 and Fig. 7.10 shows the impact of the ghost waveguide coupling coefficient ϵ_2 on the phase transfer function ϕ_r. In these graphs, the phase transfer function ϕ_r is plotted against the normalized frequency βL and graphs are plotted for various values of ϵ_2. The value of ϵ_1 in both graphs is 0.5 but $a = 1$ i.e. lossless device for the graph in Fig 7.9 and $a = 0.95$ for the graph in Fig 7.10.

As seen in Fig 7.9, the phase transfer function ϕ_r changes very gradually as ϵ_2 increases. Even introducing loss in the device by using $a = 0.95$ for the graph in Fig/ 7.10, there is no visible change in the graph comparing to Fig. 7.9.

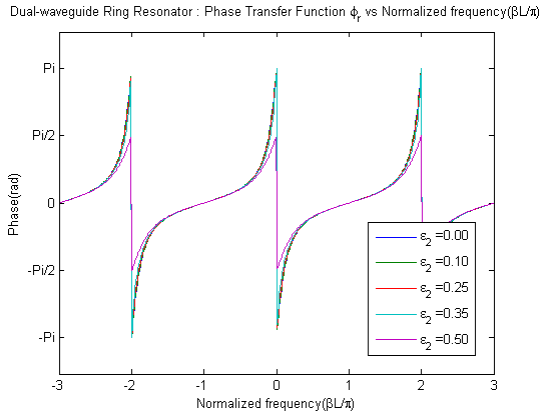

Figure 7.9: Phase Transfer Function ϕ_r vs. ϵ_1

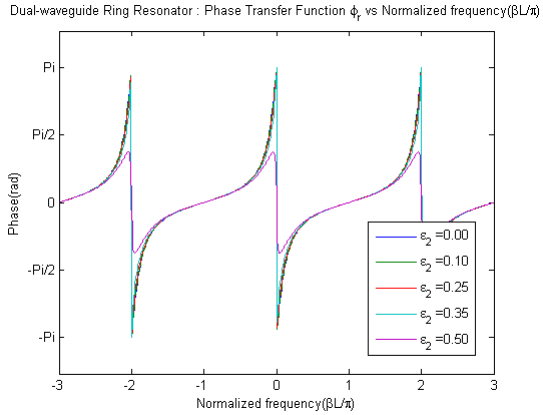

Figure 7.10: Phase Transfer Function ϕ_r vs. ϵ_1

7.6.3 Performance Parameters Spectra with MATLAB for $\epsilon_2 = 0$

The above performance parameters are plotted with the MATLAB using equations (7.14), (7.15), (7.16). But these graphs can be plotted directly using the transfer matrices of basic building blocks of ring resonator i.e. rotated directional coupler and parallel waveguides. The matrix multiplication of RDC1, PWG and RDC2 can be done in MATLAB and the performance parameters can be calculated and plotted in MATLAB directly. But we can't use $\epsilon_2 = 0$ in the MATLAB as it gives an error for RDC2 transfer matrix because of presence of $\epsilon_2 = 0$ in denominator. We can use $\epsilon_2 = 0.000001$ as this is a very small value.

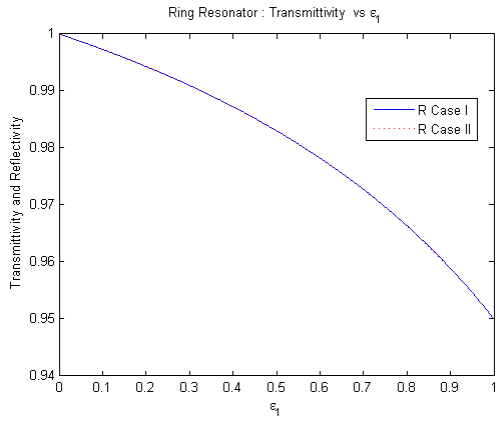

Figure 7.11: Reflectivity R vs. ϵ_1

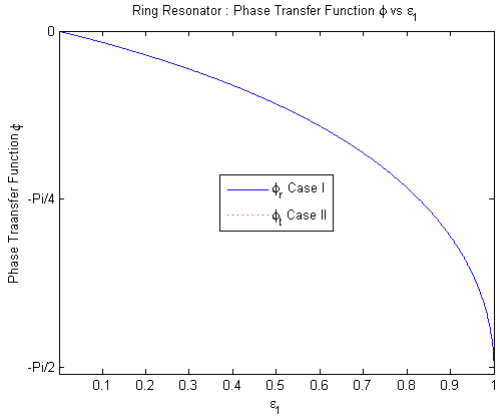

Figure 7.12: Phase Transfer Function ϕ_r vs. ϵ_1

The graphs shown in Fig. 7.11 and Fig. 7.12 have two cases. Case I graph is plotted using the equations (7.14), (7.15), (7.16). Case II graph is plotted using ϵ_2 value as 0.000001 in a matrix multiplication of RDC1, PWG and RDC2 in the MATLAB, as explained above. From Fig. 7.11 and Fig. 7.12, it can be observed that there is no difference between reflectivity as well as phase transfer function for both cases. So the use of $\epsilon_2 = 0.000001$ for ghost waveguide coupling coefficient has no effect on the output of the ring resonator.

Chapter 8

Multi-Ring Ring Resonator

8.1 Introduction

Multi-ring resonators are ring resonators with additional rings cascaded to the present ring. As number of rings increases in the multi-ring resonator, varying the coupling coefficients between the rings, many interesting devices can be formed. For the analysis of transfer functions of the multi-ring resonators, if the modeling of these devices is attempted with the help of method of equating fields or method of unfolded equivalent system, then it is very tedious and may be impossible attempt. But as explained in the chapter 6, these devices can be designed by the concatenation of the rotated directional couplers with the help of parallel waveguides. The concept of the ghost waveguides explained in chapter 7 can be used if multi-ring waveguide is not a dual-waveguide device. Analysis of the 2-ring ring resonator is explained in next section.

8.2 2-Ring Ring Resonator

The 2-ring ring resonator is similar to the ring resonator with a additional ring. The 2-ring ring resonator can be designed, as shown in Fig. 8.1, by placing additional photonic ring near the existing photonic ring creating the coupling region between two rings. Similar device is also seen in Ref. [8] as serially coupled double ring resonator. This device is has two rings and two waveguides. So this device is similar to the dual-waveguide ring resonator with two rings. 2-Ring ring resonator is also the dual-waveguide ring resonator with two rings when we uses the ghost waveguide with it. Eventually the ghost waveguide

will be eliminated.

As seen in Fig. 8.1, there are two ports in the device. When the light is entered in the input port as seen in Fig. 8.1,it travels towards the coupling region with the coupling coefficient ϵ_1. When it reaches the coupling region with the coupling coefficient ϵ_1, some quantity of the power from the input port is coupled into the ring 1 and the remaining power is dissipated at the throughput port. The power coupled into the ring 1 travels in the ring 1 till it reaches the coupling region with the coupling coefficient ϵ_2. When it reaches the coupling region with the coupling coefficient ϵ_2, some quantity of the power from the input port is coupled into the ring 2 and the remaining power is dissipated into the ring 1. So the power coupled into the ring 2 travels in the ring 2 till it reaches back to the coupling region the with coupling coefficient ϵ_2. When it reaches the coupling region with the coupling coefficient ϵ_2, it is combined with the power which comes from the ring 1. From this combined power, some quantity of the power is coupled into the ring 2 and the remaining power is coupled into the ring 1. The power coupled in the ring 1 travels till it reaches the coupling region with the coupling coefficient ϵ_1. When it reaches the coupling region with the coupling coefficient ϵ_1, it is combined with the input. Some quantity of this combined power is coupled back into the ring 1 and the remaining power is dissipated at the throughput port. The some quantity of power keeps circulating in the ring 1 and the ring 2 which generates resonances.

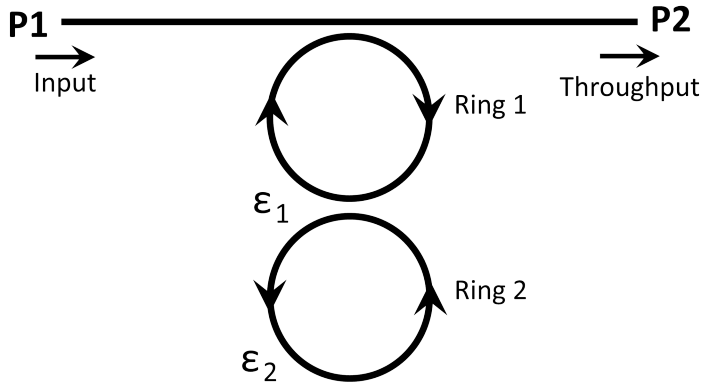

Figure 8.1: 2-Ring Ring Resonator

As the concept of the rotated directional coupler with the ghost waveguide is used for the ring resonator in previous chapter, same concept can be used for the 2-ring ring resonator. So rotating Fig. 8.1 by 90^o in counter clockwise direction, and using the concept of rotated directional coupler and parallel waveguides, similar to chapter 7, Fig. 8.2 is obtained.

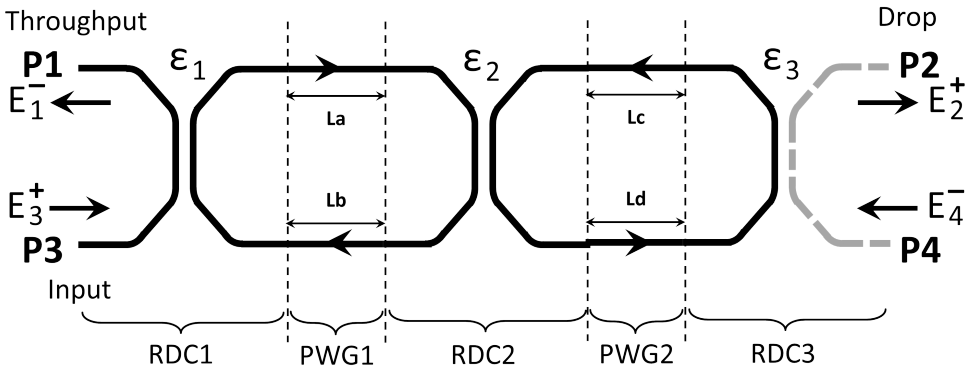

Figure 8.2: 2-Ring Ring Resonator with Ghost Waveguide

As seen in Fig. 8.2, in the 2-ring ring resonator with the ghost waveguide, RDC1 is concatenated by PWG1 which is cascaded by RDC2 which is concatenated to PWG2 and finally concatenated to RDC3. Consider the transfer matrix of 2-Ring Ring Resonator, RDC1, PWG1, RDC2, PWG2 and RDC3 is TM_{2RR}, TM_{RDC1}, TM_{PWG1}, TM_{RDC2}, TM_{PWG2} and TM_{RDC3} respectively. So the transfer matrix of the 2-Ring Ring Resonator TM_{2RR} can be calculated by the matrix multiplication of TM_{RDC1}, TM_{PWG1}, TM_{RDC2}, TM_{PWG2} and TM_{RDC3} from right to left in Fig. 8.2 as follow;

$$T_{2RR} = [TM_{RDC3}][TM_{PWG2}][TM_{RDC2}][TM_{PWG1}][TM_{RDC1}]. \tag{8.1}$$

As RDC3 is the last rotated directional coupler which is created by the ghost waveguide. So the coupling coefficient of the RDC3 i.e. ϵ_3 will be 0 for the elimination of the ghost waveguide. As discussed in the previous chapter, the performance parameters of the 2-ring ring resonator can be plotted using the MATLAB and the coupling coefficient for the ghost

waveguide i.e. $\epsilon_3 = 0.000003$. So using MATLAB program, performance parameters of the 2-ring ring resonators are plotted.

8.3 Reflection Parameter Spectra

8.3.1 Reflectivity Spectra

As the reflectivity of the ring resonator is dependent upon various parameters such as ϵ_1, α, β and L, similarly the reflectivity of the 2-ring ring resonator may be dependent upon various parameters. The following various graphs shows how the reflectivity varies with different parameters.

Reflectivity vs. ϵ_1

The graph in Fig. 8.3 shows how the reflectivity R varies with ϵ_1. For this graph, ϵ_1 is varied and other values used are $\epsilon_2 = 0.5$, $\beta L = \frac{\pi}{2}$ and $a = 0.95$.

As seen in Fig. 8.3, R decreases gradually as ϵ_1 increases. Also it can be observed that T remains 0 independent of value of ϵ_1.

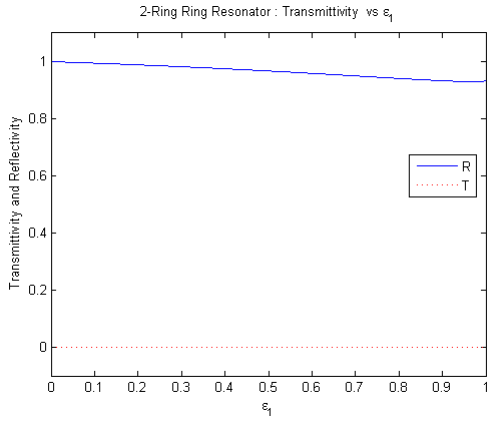

Figure 8.3: Reflectivity vs. ϵ_1

Reflectivity vs. ϵ_2

The graph in Fig. 8.4 hows how the reflectivity R varies with ϵ_2. For this graph, ϵ_2 is varied and other values used are $\epsilon_1 = 0.5$, $\beta L = \frac{\pi}{2}$ and $a = 0.95$.

As seen in Fig. 8.4, R decreases gradually as ϵ_2 increases until ϵ_2 reaches 0.8. As ϵ_2 reaches around 0.8, the R decreases very rapidly. It can be observed that T remains 0 independent of value of ϵ_2.

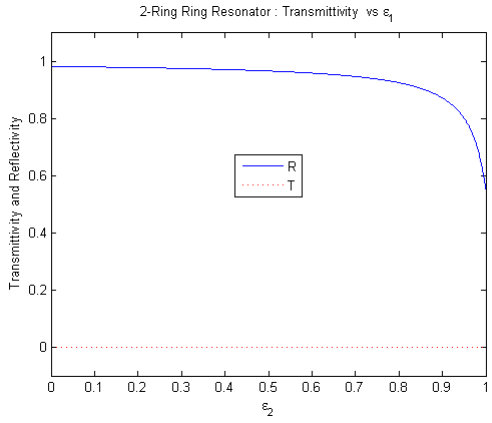

Figure 8.4: Reflectivity vs. ϵ_2

Reflectivity vs. $\frac{\beta L}{\pi}$ **- For various values** ϵ_1

The graph in Fig. 8.5 hows how the reflectivity R varies with $\frac{\beta L}{\pi}$. For this graph, ϵ_1 is varied and other values used are $\epsilon_2 = 0.5$ and $a = 0.95$.

As seen in Fig. 8.5, ϵ_1 decreases the resonances becomes sharper.The periodicity of the resonances remains same even value of ϵ_1 changes.

Reflectivity vs. $\frac{\beta L}{\pi}$ **- For various values** ϵ_2

The graph in Fig. 8.6 hows how the reflectivity R varies with $\frac{\beta L}{\pi}$. For this graph, ϵ_2 is varied and other values used are $\epsilon_1 = 0.5$ and $a = 0.95$.

As seen in Fig. 8.6, ϵ_2 changes the periodicity of the resonances. But the depth and the amplitude of resonances remains same even value of ϵ_2 changes.

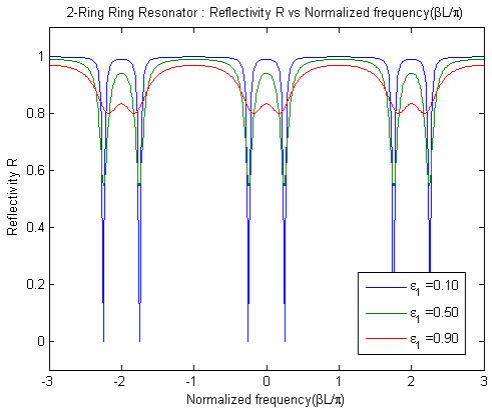

Figure 8.5: Reflectivity vs. $\frac{\beta L}{\pi}$

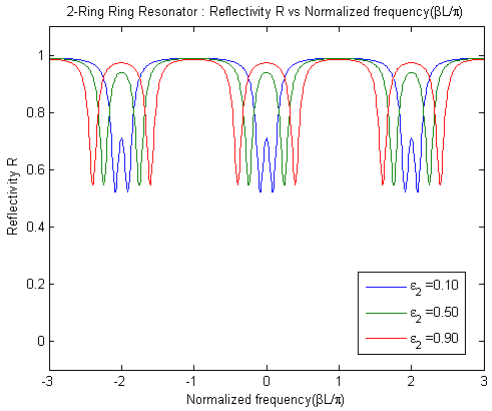

Figure 8.6: Reflectivity vs. $\frac{\beta L}{\pi}$

8.3.2 Phase Transfer Function Spectra

As the phase transfer function of the ring resonator is dependent upon various parameters such as ϵ_1, α, β and L, similarly the phase transfer function of the 2-ring ring resonator may be dependent upon various parameters. The following various graphs shows how the phase transfer function varies with different parameters.

Phase Transfer Function vs. ϵ_1

The graph in Fig. 8.7, shows how the phase transfer function varies with ϵ_1. For this graph, only ϵ_1 is varied and other values used are $\epsilon_2 = 0.5$, $\beta L = \frac{\pi}{2}$ and $a = 0.95$.

As seen in Fig. 8.7, phase ϕ_r changes from 0 to $-\frac{\pi}{2}$ as ϵ_1 increases.

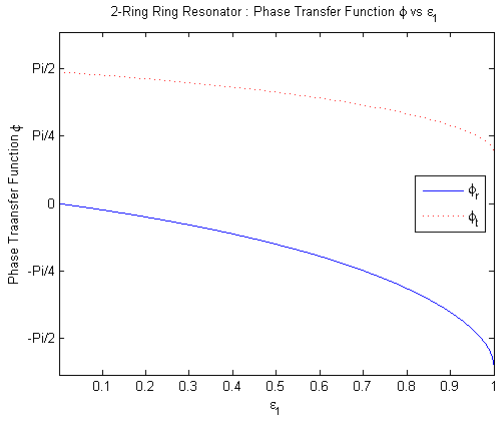

Figure 8.7: Phase Transfer Function vs. ϵ_1

Phase Transfer Function vs. ϵ_2

The graph in Fig. 8.8, shows how the phase transfer function varies with ϵ_1. For this graph, only ϵ_2 is varied and other values used are $\epsilon_1 = 0.5$, $\beta L = \frac{\pi}{2}$ and $a = 0.95$.

As seen in Fig. 8.8, phase ϕ_r changes from 0 to $-\frac{\pi}{2}$ as ϵ_2 increases.

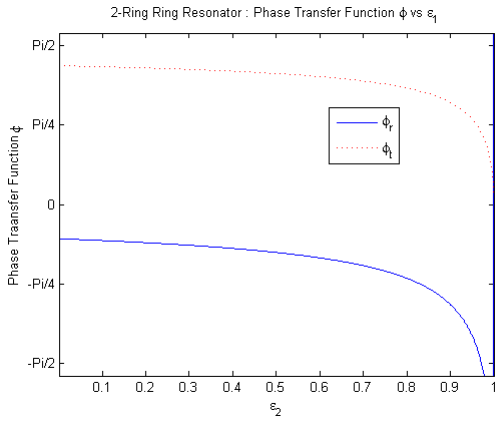

Figure 8.8: Phase Transfer Function vs. ϵ_2

Phase Transfer Function ϕ_r **vs.** $\frac{\beta L}{\pi}$ **- For various values** ϵ_1

The graph in Fig. 8.9, shows how the phase transfer function varies with $\frac{\beta L}{\pi}$. For this graph, ϵ_1 is also varied and other values used are $\epsilon_2 = 0.5$ and $a = 0.95$.

As seen in Fig. 8.9, it can be observed that the frequecncy of resonances remains same even the value of ϵ_1 changes. The phase changes very gardually with change in ϵ_1.

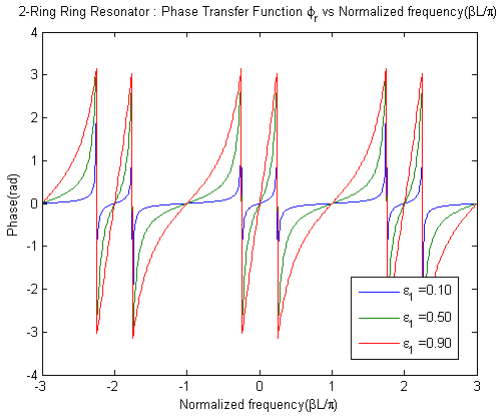

Figure 8.9: Phase Transfer Function ϕ_r vs. $\frac{\beta L}{\pi}$

Phase Transfer Function ϕ_r vs. $\frac{\beta L}{\pi}$ - For various values ϵ_2

The graph in Fig. 8.10, shows how the phase transfer function varies with $\frac{\beta L}{\pi}$. For this graph, ϵ_2 is also varied and other values used are $\epsilon_1 = 0.5$ and $a = 0.95$.

As seen in Fig. 8.10, it can be observed that the frequency of resonances remains changes as ϵ_2 changes.

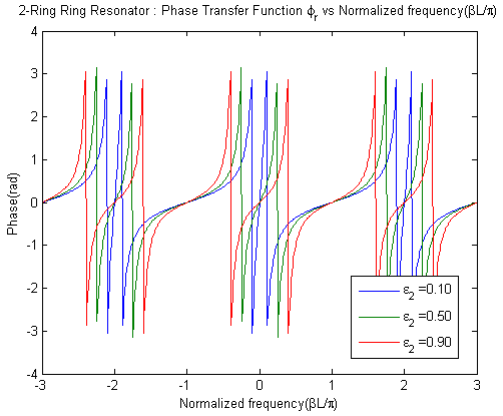

Figure 8.10: Phase Transfer Function ϕ_r vs. $\frac{\beta L}{\pi}$

8.4 Modeling of Multi-Ring Resonators

As discussed previously, multi-ring ring resonators analysis gets complicated and tedious as the number of rings increases. As seen in chapter 2, the analysis of 2-ring ring resonator using the method of equating fields or the method of unfolded equivalent system is complicated. But previous section demonstrates that the analysis of the 2-ring ring resonator by new technique of ghost waveguides is not complicated. New technique used with MATLAB makes the analysis of multi-ring ring resonators simple.

Chapter 9

Conclusion

This thesis explored a method of modeling and analyzing photonic loop structures which is based on rotated directional coupler with a ghost waveguide.

As the photonic directional coupler, photonic rotated directional coupler and photonic parallel waveguides are basic building blocks of our technique, we first derived the scattering matrix and transfer matrix of a directional coupler. By rotating the directional coupler by 90^o counter-clockwise, we achieved the rotated directional coupler and derived its scattering matrix and transfer matrix. Even though the functionality of a rotated directional function is same as a directional coupler, its application is different. The scattering matrix and transfer matrix for parallel waveguides have been derived. We introduced the concept of ghost waveguides which are not existing in the photonic device but can be used as convenience for the purpose of simplification of modeling and analysis of the device. The concept of a ghost waveguide is demonstrated for rotated directional coupler.

We modeled and analyzed the dual-waveguide ring resonator. Rotated directional couplers are concatenated with parallel waveguides which again are concatenated to rotated directional couplers and the method of transfer matrix multiplication is used to get the transfer matrix of the dual-waveguide ring resonator. The analysis of the dual-waveguide ring resonator verifies the method of concatenation of basic building blocks of the photonic-loop structures and that the transfer matrix multiplication method can be used for photonic-loop structures.

We then modeled and analyzed the ring resonator with the help of a rotated directional coupler with ghost waveguide. By introduction of the ghost waveguide,the ring resonator

becomes a dual-waveguide ring resonator and the results from the dual-waveguide ring resonator are used as a starting point for ring resonator modeling. Later by excluding the ghost waveguide, the results of the ring resonator is obtained. These results are verified with the available results. So modeling and analysis of the ring resonator is authenticated by the method of photonic-loop modeling using ghost waveguides. Later we extended this method for a 2-ring ring resonator analysis using MATLAB.

A new method of modeling with ghost waveguides can be useful for photonic-loop structures especially considering compound structures. The concept of ghost waveguides can also be used in other photonic structures apart from loop structures.

Bibliography

[1] G.P. Agrawal. *Lightwave Technology*. John Wiley & Sons, Inc., Hoboken,New Jersey, 2004.

[2] J. Capmany and M.A. Muriel. A new transfer matrix formalism for the analysis of fiber ring resonators: compound coupled structures for fdma demultiplexing. *Lightwave Technology, Journal of*, 8(12):1904–1919, 1990.

[3] John E. Heebner and Robert W. Boyd. Enhanced all-optical switching by use of a nonlinear fiber ring resonator. *Opt. Lett.*, 24(12):847–849, Jun 1999.

[4] Jurgen Jahns and Karl-Heinz Brenner. *Microoptics : From Technology to Applications*. Springer, New York, 2004.

[5] Gerd Keiser. *Optical Fiber Communications*. Mc Graw Hill, New York, 2011.

[6] R. Marz and G. Hilliger. On the transfer matrix theory of contradirectional devices. *Optical and Quantum Electronics*, 32(6-8):829–842, 2000.

[7] Reinhard Marz. *Integrated Optics : Design and Modeling*. Artech House, Boston, 1995.

[8] D.G. Rabus. *Integrated Ring Resonators : The Compendium*. Springer, Berlin, 2007.

[9] Paul Urquhart. Transversely coupled fiber fabry-perot resonator: theory. *Appl. Opt.*, 26(3):456–463, Feb 1987.

[10] Paul Urquhart. Compound optical-fiber-based resonators. *J. Opt. Soc. Am. A*, 5(6):803–812, Jun 1988.

[11] A. Yariv. Universal relations for coupling of optical power between microresonators and dielectric waveguides. *Electronics Letters*, 36(4):321–322, 2000.

[12] Jianluo Zhang and John W. Y. Lit. Compound fiber ring resonator: theory. *J. Opt. Soc. Am. A*, 11(6):1867–1873, Jun 1994.